Quantum entanglement entropy and classical mutual information in long-range harmonic oscillators

M. Ghasemi Nezhadhaghighi[1,2] and M. A. Rajabpour[3,*]

[1]*Department of Physics, Sharif University of Technology, Tehran, P.O. Box 11365-9161, Iran*

[2]*Institute for Physics and Astronomy, University of Potsdam, 14476 Potsdam-Golm, Germany*

[3]*Instituto de Física de São Carlos, Universidade de São Paulo, Caixa Postal 369, 13560-970 São Carlos, SP, Brazil*

(Received 1 April 2013; published 16 July 2013)

We study different aspects of quantum von Neumann and Rényi entanglement entropy of one-dimensional long-range harmonic oscillators that can be described by well-defined nonlocal field theories. We show that the entanglement entropy of one interval with respect to the rest changes logarithmically with the number of oscillators inside the subsystem. This is true also in the presence of different boundary conditions. We show that the coefficients of the logarithms coming from different boundary conditions can be reduced to just two different universal coefficients. We also study the effect of the mass and temperature on the entanglement entropy of the system in different situations. The universality of our results is also confirmed by changing different parameters in the coupled harmonic oscillators. We also show that more general interactions coming from general singular Toeplitz matrices can be decomposed to our long-range harmonic oscillators. Despite the long-range nature of the couplings, we show that the area law is valid in two dimensions and the universal logarithmic terms appear if we consider subregions with sharp corners. Finally, we study analytically different aspects of the mutual information such as its logarithmic dependence to the subsystem, effect of mass, and influence of the boundary. We also generalize our results in this case to general singular Toeplitz matrices and higher dimensions.

DOI: 10.1103/PhysRevB.88.045426 PACS number(s): 05.30.−d

I. INTRODUCTION

Quantum entanglement entropy as an interesting quantity in many-body systems has been studied in many different locally interacting systems by using different techniques, see the reviews in Refs. 1–6 and references therein. Among the most important results (which are related to this work), one can list the classical work of Bombelli *et al.*,[7] where they compute the entanglement entropy of free field theory by using the discrete version of the field theory, which is simply coupled harmonic oscillators. The result was rediscovered in Ref. 8 and used to introduce the area law. In Ref. 9, the result was generalized to the Rényi entropy and the validity of the replica trick is checked. This method is also used to study free fermionic systems in a series of papers by Peschel and collaborators in Refs. 6 and 10. The techniques used in these works are applicable in any dimension. In two dimensions for the short-range interacting systems, one can also derive exact formulas for the entanglement entropy using Euclidean methods.[5] In the especial cases when one has integrable models, one can use the form factor techniques and calculate the entanglement entropy.[11] Finally, at the quantum critical point when we use conformal field theory, many explicit results are known, see Ref. 4 and references therein.

Although in short-range interacting systems numerous results have been discovered in the last ten years, there are just few results concerning long-range interacting systems. The main difficulty is the lack of exact solution in most of this kind of systems. The entanglement entropy in Lipkin-Meshkov-Glick (LMG) model, where all spins interact among themselves, is studied numerically and analytically in Refs. 12 and 13. In Ref. 14, the static and the dynamical properties of the entanglement entropy are studied in a long-range Ising type model without an external magnetic field. In the same direction, the entanglement entropy is also calculated numerically for the antiferromagnetic long-range Ising chain in Ref. 15. In an interesting work, see Ref. 16, a logarithmically divergent geometric entropy is found in free fermions with long-range unshielded Coulomb interaction. Plenio *et al.*,[17–19] see also Refs. 20 and 21, studied the general properties of the entanglement entropy for coupled harmonic oscillators and found an interesting bound for the entanglement entropy. Finally, using the matrix product states, it was argued in Ref. 22 that for those long-range systems that one can not approximate the ground state of the model with the ground state of another short-range model, we expect larger entanglement. One can find some other results concerning entanglement entropy in long-range systems in Ref. 23.

Recently, using the methods of Refs. 7 and 9, we studied the entanglement entropy of a block of long-range coupled harmonic oscillators.[24] We showed that the entanglement of the gapless system is logarithmically dependent on the system size, and we calculated the prefactor of the logarithm in different situations. The idea of studying this particular nonlocal system is manyfold: firstly, the Hamiltonian (1), which we are going to study, is a simple discretization of fractional Laplacian, and therefore, it has a very clean continuum limit. This is useful because then we can claim that we are actually studying the entanglement entropy of a nonlocal field theory. This field theory is a well-known field theory, which also appears in the study of long-range Ising model,[25] so in principle, any analytical understanding of the entanglement entropy of long-range Ising model will be based on the system that we are studying. Having the above motivations in mind, we extended our study in many different directions.

The organization of the paper is as follows. In Sec. II, we present the model and give the definitions of the quantities that we are going to study. In Sec. III, we study different aspects of von Neumann and Rényi entanglement entropy in long-range harmonic oscillators. We first summarize the main formulas that we need to calculate the entanglement

entropy. Most of the formulas are in the discrete level but we also provide the eigenvalue problems in the continuum limit. Then we study the entanglement entropy numerically both at the purely discrete level and also at the level of discretization of the eigenvalue problem. This part of the paper is the extension of the work done in Ref. 24. Then we study the finite size effects in different kinds of situations such as, periodic and Dirichlet boundary conditions. Then, we compare the results with the massive coupled long-range oscillators. After that, we study the effect of temperature on the entanglement entropy of our system. Our main result will be presented at the end of this section, which concerns the universality of our results. In this section, we will show that the results presented in the previous sections are robust against many small changes in the form of the interaction. We will also show that one can calculate the entanglement entropy of a larger set of coupled oscillators, to be specific, oscillators coupled with singular Toeplitz interactions, to the cases that we studied in previous sections. We will conclude this section with some comments about the entanglement entropy in higher dimensions, especially, in the presence of polygonal regions. Finally, in Sec. IV, we will study different aspects of the classical mutual information in long-range harmonic oscillators. We will presents two definitions, and then using the Fisher-Hartwig theorem, we will show that in contrast to the von Neumann entanglement entropy one can actually analytically calculate these quantities. In this section, we also address the finite size effects and also the massive case. The generalization to the singular Toeplitz matrices will be also discussed.

II. DEFINITIONS AND SETTINGS

We start by describing the coupled harmonic oscillators, perhaps the simplest lattice model available where the Hamiltonian is a quadratic form:

$$\mathcal{H} = \frac{1}{2}\sum_{n=1}^{N} \pi_n^2 + \frac{1}{2}\sum_{n,n'=1}^{N} \phi_n K_{nn'} \phi_{n'}. \tag{1}$$

We would like to study coupled harmonic oscillators with long-range interaction. To define the K matrix for the long-range harmonic oscillator problem, one can use the fractional operator. In principle, there are many ways to write a long-range K matrix, however, we are interested in those that have a very simple continuum counterpart. In principle, in the continuum, the fractional Laplacian is usually defined by its Fourier transform $|q|^\alpha$ or $(q^2)^{\frac{\alpha}{2}}$, where q^2 is just the Fourier transform of a simple Laplacian. Since the Fourier transform of the discrete Laplacian is $2-2\cos q$, one may use some powers of this to define the discrete fractional Laplacian. Then, the elements of the matrix K, representing the discretized fractional Laplacian, are

$$\begin{aligned} K_{l,m} &= -\int_0^{2\pi} \frac{dq}{2\pi} e^{iq(l-m)} \left(\{2[1-\cos(q)]\}^{\frac{\alpha}{2}} + M^\alpha \right) \\ &= \frac{\Gamma\left(-\frac{\alpha}{2}+n\right)\Gamma(\alpha+1)}{\pi\Gamma\left(1+\frac{\alpha}{2}+n\right)} \sin\left(\frac{\alpha}{2}\pi\right) + M^\alpha \delta_{l,m}, \end{aligned} \tag{2}$$

where $n = |l-m|$ and fractional order $\alpha > 0$. In the future, M will play the role of the mass of the fractional field theory. In the special case $\alpha = 2$, the K matrix is equal to the simple Laplacian. When $\alpha/2$ is an integer, the elements $K(n) = (-1)^{\alpha-n+1} C_{\alpha,\frac{\alpha}{2}+n}$ for $n \leqslant \alpha/2$ and $K(n) = 0$ for $n > \alpha/2$, where $C_{\alpha,\frac{\alpha}{2}+n}$ are binomial coefficients.[26]

For a sufficiently large one-dimensional system, K and the two-point correlator matrices $K^{\pm 1/2}$ are Toeplitz matrices, and all their off-diagonal elements are identical. The elements of $K^{\pm 1/2}_{l,m}$ can be expressed as a Fourier series

$$\begin{aligned} K^{\pm 1/2}_{l,m} &= K^{\pm 1/2}(n) \\ &= -\int_0^{2\pi} \frac{dq}{2\pi} e^{iq(l-m)} \left(\{2[1-\cos(q)]\}^{\frac{\alpha}{2}} + M^\alpha \right)^{\pm 1/2}. \end{aligned} \tag{3}$$

The matrix $K^{-1/2}$ corresponds to the spatial correlation of an oscillator system $\langle \phi_l \phi_m \rangle$, and for the system with periodic boundary condition, one can find the spatial correlation length ξ_s as[27]

$$\begin{aligned} \xi_s^{-1} &\equiv -\lim_{n\to\infty} \frac{1}{n} \log |\langle \phi_l \phi_{l+n} \rangle| \\ &= -\lim_{n\to\infty} \frac{1}{n} \log |K^{-1/2}(n)|. \end{aligned} \tag{4}$$

For the massless system, $\xi_s^{-1} = -\lim_{n\to\infty} \frac{1}{n} \log \left| \frac{\Gamma(n+\alpha/4)\Gamma(1-\alpha/2)}{\pi\Gamma(1-\alpha/4+n)} \sin(\frac{\alpha}{4}\pi) \right| = 0$ and for the massive case, $\xi_s^{-1} \propto M$. We note that for $M = 0$, the correlation length ξ_s is infinite and the system is gapless, and for nonzero value of M, the system is gapped.

The K matrix in the continuum limit has the following form:

$$\begin{aligned} &\frac{1}{2}\sum_{n,n'=1}^{N} \phi_n K_{nn'} \phi_{n'} \\ &\quad \to \int \left[-\frac{1}{2}\phi(x)(-\nabla)^{\alpha/2}\phi(x) + \frac{1}{2}M^\alpha \phi^2(x) \right] dx, \end{aligned} \tag{5}$$

where $-(-\nabla)^{\alpha/2}$ is defined by its Fourier transform $|q|^\alpha$.

We are now in a position to introduce the entanglement entropy and its value in two-dimensional conformal field theories (CFT's). Here, we shall only discuss the von Neumann and Rényi entanglement entropies. Nevertheless, there are many other measures that have been explored[1–3].

Consider a system with the density matrix of a pure state ρ, which is divided into two subsystems A and B. Then the entanglement may be characterized by the properties of the reduced density matrix ρ_A of the subsystem A. Density matrix ρ_A is obtained by tracing out the remaining degrees of freedom $\rho_A = \mathrm{tr}_B \rho$. The von Neumann entanglement entropy associated to the local density matrix ρ_A reduced to a region A of the space is

$$S(A) = -\mathrm{tr}[\rho_A \log(\rho_A)]. \tag{6}$$

Another measure, related to the local density matrix, is a family of functions called the Rényi entropies:

$$S_n(A) = \frac{1}{1-n} \log\left(\mathrm{tr}\rho_A^n\right), \quad n \geqslant 0, \quad n \neq 1. \tag{7}$$

The Rényi entropy S_n has similar properties as the entanglement entropy S.

For general quantum field theories in d spatial dimensions, the entanglement entropy is always divergent in a continuum system and the coefficient of the leading divergence term is proportional to the area of the boundary of the subsystem A, and it is given by the simple formula[5]

$$S(A) = g_{d-1}\left(\frac{l}{\epsilon}\right)^{d-1} + \cdots + g_1\left(\frac{l}{\epsilon}\right)^{1} + g_0 \log(l/\epsilon) + S_0(A), \tag{8}$$

where $\{g_{d-1}, \ldots, g_1\}$ and S_0 are nonuniversal constants that depend on the system. The coefficient g_0 of the logarithm term is expected to be universal, l^d is the volume in d-dimensional space, and ϵ is a short distance cutoff (or a lattice spacing). The simple area law, however, can not describe the scaling of the entanglement entropy in generic cases. Indeed, the entanglement entropy of conformal field theory in one special dimension scales logarithmically with respect to the size of the subsystem l. If the total system is infinitely long, it is given by the simple formula

$$S = \frac{c}{3}\log\frac{l}{\epsilon}, \tag{9}$$

where c is the central charge of the CFT[28]. In $1+1$-dimensional conformal invariant systems, the Reńyi entropy is[31]

$$S_n = \frac{c}{6}\left(1+\frac{1}{n}\right)\log\frac{l}{\epsilon}. \tag{10}$$

It is also worth mentioning that at zero temperature and one special dimension, for a finite system of length L with boundary divided into two pieces of lengths l and $L-l$, the Rényi entropy obeys

$$S_n = \frac{c}{12}\left(1+\frac{1}{n}\right)\log[(L/\pi a)\sin(\pi l/L)] + c_1'. \tag{11}$$

The above formulas are a few among many others that are known for different cases in two-dimensional CFT's, see Ref. 4. In the next sections, we will introduce many of them as the limiting behavior of our long-range harmonic oscillators.

In the next section, we will review a method where one can use it to calculate ρ_A and consequently S and S_n for generic quadratic bosonic systems. Then, we will hire this technique to study our particular long-range system.

III. VON NEUMANN AND RÉNYI ENTANGLEMENT ENTROPY

A. Hamiltonian approach

A useful method to obtain entanglement entropy is introduced in Ref. 7, rediscovered in Ref. 8, and generalized to Rényi entropy in Ref. 9. In this method, one would like to measure the quantum entanglement entropy of the ground state of the free field $\{\phi\}$, generated by tracing over fields inside the region of the boundary surface. To fix the notation and for later use, we give here a brief summary of the work described in more detail in Refs. 7 and 9. The ground-state wave functional is given by

$$\Psi_0(\{\phi\}) \propto (\det\Gamma)^{\frac{1}{4}} \exp\left(-\sum_{n,n'=1}^{N}\phi_n\Gamma_{nn'}\phi_{n'}\right), \tag{12}$$

where $\{\phi\}$ denotes the collection of all ϕ's, one for each oscillator and $\Gamma = K^{1/2}$.

Now consider a subregion in the total space and split the field variables into inside ($\{\phi\}_A$) and outside ($\{\phi\}_B$) parts, then one can rewrite the ground-state wave function as

$$\Psi_0 \propto \exp\left[-(\{\phi\}_A\{\phi\}_B)\begin{pmatrix}\Gamma_{AA} & \Gamma_{AB}\\ \Gamma_{BA} & \Gamma_{BB}\end{pmatrix}\begin{pmatrix}\{\phi\}_A\\ \{\phi\}_B\end{pmatrix}\right], \tag{13}$$

where $\Gamma_{\oplus\otimes}$ ($\oplus = \{A,B\}$ and $\otimes = \{A,B\}$) denotes the kernel matrix restricted to the inside or the outside.

For the fields $\{\phi^{1,2}\}_A$, which are defined in the inside region, the ground-state density matrix $\rho_A(\{\phi^1\}_A,\{\phi^2\}_A)$ is given by

$$\rho_A(\{\phi^1\}_A;\{\phi^2\}_A) \propto (\det(\Gamma_{AA})^{-1})^{\frac{1}{2}} \exp\left[-\frac{1}{2}(\{\phi^1\}_A\{\phi^2\}_A) \times \begin{pmatrix}\mathcal{A} & 2\mathcal{B}\\ 2\mathcal{B} & \mathcal{A}\end{pmatrix}\begin{pmatrix}\{\phi^1\}_A\\ \{\phi^2\}_A\end{pmatrix}\right], \tag{14}$$

where

$$\mathcal{A} = 2\left[\Gamma_{AA} - \tfrac{1}{2}\Gamma_{AB}(\Gamma_{BB})^{-1}\Gamma_{BA}\right],\qquad \mathcal{B} = -\frac{1}{2}\Gamma_{AB}(\Gamma_{BB})^{-1}\Gamma_{BA}. \tag{15}$$

From now on, one can follow two different methods to get the entanglement entropy: one is based on direct diagonalization of the above reduced density matrix and the other based on using a replica trick. For later use, we will summarize the results for both of them. Using appropriate transformations,[7] one can write the reduced density matrix as

$$\rho_A(\{\phi^1\}_A;\{\phi^2\}_A) = \prod_i \frac{1}{\sqrt{\pi}}\exp\left[-\frac{1}{2}\left(\phi_n^1\phi^{1n}+\phi_n^2\phi^{2n}\right) - \frac{1}{4}E_i(\phi^1-\phi^2)_n(\phi^1-\phi^2)^n\right], \tag{16}$$

where E_i's are the eigenvalues of the matrix Λ with the following simple form:

$$\Lambda \equiv -(\Gamma^{-1})_{AB}\Gamma_{BA}. \tag{17}$$

The interesting point about Eq. (16) is that it has the form of the reduced density matrix of a two-body harmonic oscillator. In other words, for the ground state of a coupled harmonic oscillator, the problem of calculating the entanglement entropy can be reduced to the problem of calculating the entanglement entropy of two coupled harmonic oscillators. One can then show that the entropy can be expressed in terms of the eigenvalues E_i of Λ as[7]

$$S = \sum_i\left[\log\frac{\sqrt{E_i}}{2} + \sqrt{1+E_i}\log\left(\frac{1}{\sqrt{E_i}} + \sqrt{1+\frac{1}{E_i}}\right)\right]. \tag{18}$$

It is worth mentioning that having larger coupling between two oscillators leads to larger E and, consequently, larger entanglement entropy.

The second method, which is also useful to get the Rényi entropy, is based on the replica trick. Using Eq. (14) and rescaling the reduced density matrix, one can calculate $\mathrm{tr}\rho_A^n$ and ultimately the entropy[9] as the following sum:

$$S = \lim_{n\to 1} \frac{1}{1-n} \log\left(\mathrm{tr}\rho_A^n\right) = -\sum_{i=1}^{l} \left[\ln(1-\xi_i) + \frac{\xi_i}{1-\xi_i}\ln\xi_i\right], \tag{19}$$

where ξ_i is related to the eigenvalue of the matrix $\mathcal{C} = -2\mathcal{A}^{-1}\mathcal{B}$ by $\mathcal{C}_i = \frac{2\xi_i}{1+\xi_i^2}$.

It is also useful to consider the matrix $\Lambda = (1-\mathcal{P})^{-1}\mathcal{P}$ where $\mathcal{P} \equiv \Gamma_{AA}^{-1}\Gamma_{AB}\Gamma_{BB}^{-1}\Gamma_{BA}$, which has also the simple form (17) and write Eq. (19) in terms of eigenvalues of the matrix Λ as Eq. (18). The eigenvalues E_i of the matrix Λ are positive and related to ξ_i by

$$\xi_i = \frac{\sqrt{1+E_i}-1}{\sqrt{1+E_i}+1}. \tag{20}$$

It is also straightforward to write the Rényi entropy S_n in term of ξ_i as

$$S_n = \frac{1}{n-1}\sum_i \left[\log\left(1-\xi_i^n\right) - n\log(1-\xi_i)\right]. \tag{21}$$

In order to compute the entanglement entropy obtained by tracing over the fields in the region A for a given problem, one should find the eigenvalues of the matrix Λ. For a given Hamiltonian $\mathcal{H}$, one can easily find the operators K and, consequently, Γ and Γ^{-1}. In the continuum limit, the operator Λ is obtained after integration over the oscillators in the region B as

$$\Lambda(x,y) = -\int_B dz\Gamma^{-1}(x,z)\Gamma(z,y). \tag{22}$$

The eigenvalue problem to be solved is then

$$\int dy\Lambda(x,y)\psi(y) = E\psi(x), \tag{23}$$

where $\psi(x)$ is an eigenfunction with eigenvalue E.

It is worth mentioning that for the general Hamiltonian (1), one can calculate the two-point correlators $X_A = \mathrm{tr}(\rho_A\phi_i\phi_j)$ and $P_A = \mathrm{tr}(\rho_A\pi_i\pi_j)$ using the K matrix by

$$\frac{1}{2}K^{-1/2} = \begin{pmatrix} X_A & X_{AB} \\ X_{AB}^T & X_B \end{pmatrix}, \quad \frac{1}{2}K^{1/2} = \begin{pmatrix} P_A & P_{AB} \\ P_{AB}^T & P_B \end{pmatrix}. \tag{24}$$

Then one can define matrix $C = \sqrt{X_A P_A}$, which has the eigenvalues[5]

$$\nu_i = \coth\left[-\log\left(\frac{\sqrt{1+E_i}-1}{\sqrt{1+E_i}+1}\right)\Big/2\right], \tag{25}$$

where ν_i are the eigenvalues of C. With respect to the new operators, the entropy is given by

$$\begin{aligned} S =& \ \mathrm{tr}\left[\left(C+\frac{1}{2}\right)\log\left(C+\frac{1}{2}\right) - \left(C-\frac{1}{2}\right)\log\left(C-\frac{1}{2}\right)\right] \\ =& \sum_{i=1}^{l}\left[\left(\nu_i+\frac{1}{2}\right)\log\left(\nu_i+\frac{1}{2}\right) - \left(\nu_i-\frac{1}{2}\right)\log\left(\nu_i-\frac{1}{2}\right)\right]. \end{aligned} \tag{26}$$

We also have

$$\begin{aligned} S_n =& \frac{1}{n-1}\mathrm{tr}\left\{\log\left[\left(C+\frac{1}{2}\right)^n - \left(C-\frac{1}{2}\right)^n\right]\right\} \\ =& \frac{1}{n-1}\sum_{i=1}^{l}\left\{\log\left[\left(\nu_i+\frac{1}{2}\right)^n - \left(\nu_i-\frac{1}{2}\right)^n\right]\right\}, \end{aligned} \tag{27}$$

where l is the size of the subsystem A. In this formulation, we need only the correlators inside the region A, to calculate S and S_n.

In order to clarify the Hamiltonian approach in the continuum limit, we briefly review the procedure followed in Ref. 9 to find an approximate analytical solution for the harmonic oscillator system with short-range interaction. This method is introduced in order to determine E and also S by using the eigenvalue problem (23). They considered a one-dimensional coupled harmonic oscillator with mass M, confined to the region $-L < x < L$ and the subsystem is taken to be half of a finite system.

To calculate the eigenvalue E, for a system of harmonic oscillators with short-range interactions, it is better to first consider a system with infinite size $L \to \infty$. At this limit, the kernels $\Gamma^{\pm 1}$ needed to construct E have the following forms:

$$\begin{aligned} \Gamma(x,y) &= MK_1[M(x-y)]/[\pi(x-y)], \\ \Gamma^{-1}(x,y) &= K_0[M(x-y)]/\pi, \end{aligned} \tag{28}$$

where M is the mass term. In the $M \to 0$ limit, it is easy to show that $\psi = \exp(\iota\omega\ln x)$ is an eigensolution of the Eq. (23) with eigenvalue

$$E = \sinh^{-2}(\pi\omega). \tag{29}$$

To discretize the spectrum and calculate the entropy, one needs to impose Dirichlet boundary conditions at some large $x = L$ and further Dirichlet condition at some small $x = \epsilon$. The eigenvalues and eigenvectors are then

$$\psi(x) = \sin[\omega(E)\ln(x/\epsilon)], \quad \omega(E_i)\ln(L/\epsilon) = \pi i. \tag{30}$$

It is useful to note that the density of states per unit ω interval is constant. Now one can rewrite the continuum limit of the Rényi entropy (21) and the entanglement entropy as an integral over ω,

$$S_n = \frac{\log L}{\pi(n-1)}\int_0^\infty d\omega[\log(1-\xi^n) - n\log(1-\xi)], \tag{31}$$

$$S = \frac{\log L}{\pi}\int_0^\infty d\omega\left[\frac{\xi}{\xi-1}\log(\xi) - \log(1-\xi)\right], \tag{32}$$

where $\xi(\omega)$ is defined in Eq. (20).

As discussed before, conformal invariance implies universal properties for the entanglement entropy. The entanglement entropy and also the Réyni entropy for these models, diverge logarithmically with the subsystem size with prefactors proportional to c and c_n, respectively.

By using Eq. (32) and also Eqs. (20) and (29), one can find the entanglement entropy S for the harmonic oscillator problem, giving the result $S = \frac{1}{6}\log(L/\epsilon)$, which is consistent with $c = 1$. In addition, using Eq. (31), one can also find the Rényi entropy $S_n = \frac{1}{12}(1+\frac{1}{n})\ln(L/\epsilon)$ consistent with the CFT predictions.[31]

Next, we consider a short-range harmonic oscillator with infinite size and a subsystem with length l. This kind of configuration is completely different from Ref. 9. We should remember that Eqs. (29) and (30) are no longer true in this configuration. We proceed with Eq. (22). To evaluate this integral, we must consider $B \in (-\infty < z < 0) \cup (l < z < \infty)$ as the complement of the subregion l. The matrix Λ becomes

$$\begin{aligned}\Lambda(x,y) &= -\frac{1}{\pi^2}\int_B \frac{\ln(x+z)}{(z+y)^2}dz \\ &= \frac{1}{\pi^2}\left[\frac{(l-x)\log(l-x)-(l-y)\log(l-y)}{(l-y)(y-x)}\right. \\ &\quad \left. -\frac{x\log(x)-y\log(y)}{(y-x)y}\right]. \end{aligned} \tag{33}$$

Therefore, according to Eq. (23), the eigenvalues E_i and the corresponding eigenfunctions $\psi_i(x)$ can be obtained by diagonalizing the Λ matrix. Unfortunately, we were unable to find E_i analytically. One can numerically evaluate E_i and ψ_i using direct diagonalization of the matrix Λ, then try to guess the formula for eigenvalues and eigenfunctions. We shall come to this problem in the next section by means of numerical calculations.

We are now ready to speak more about the long-range harmonic oscillator (LRHO) with $\alpha < 2$. To determine E and ψ for LRHO, we calculated first the matrices $\Gamma = K^{1/2}$ and $\Gamma^{-1} = K^{-1/2}$. The continuum limit of the matrices Γ and Γ^{-1} has the following forms:

$$\begin{aligned}\Gamma^{\pm 1}(x,y) &= \frac{1}{2\pi}\int_{-\infty}^{\infty} dk(|k|^\alpha + M^\alpha)^{\pm 1/2} e^{ik.(x-y)} \\ &= \frac{1}{2\Gamma(\mp\alpha/2)}\frac{1}{|r|^{1\pm\alpha/2}} \\ &\quad \times H_{3,2}^{1,2}\left((M|r|)^\alpha \left| \begin{matrix}(1,1)\left(\mp\frac{\alpha}{2},1\right)\left(\mp\frac{\alpha}{4},\frac{\alpha}{2}\right) \\ \left(\mp\frac{\alpha}{2},1\right)\left(\mp\frac{\alpha}{4},\frac{\alpha}{2}\right)\end{matrix}\right.\right) \\ &= \frac{1}{2\Gamma(\mp\alpha/2)\cos\left(\frac{\pi\alpha}{4}\right)}\frac{1}{|r|^{1\pm\alpha/2}} + \mathcal{O}(M^\alpha), \end{aligned} \tag{34}$$

where $r = x - y$ and $H_{3,2}^{1,2}$ is the Fox H function. Then, in a similar way as in Eq. (22), we found the matrix Λ by multiplying Γ and Γ^{-1} in the complement region $B \in (-\infty < z < 0) \cup (l < z < \infty)$ as

$$\Lambda(x,y) = \mathfrak{A}\left\{\frac{2\left[\left(\frac{l-x}{l-y}\right)^{\alpha/2} - \left(\frac{x}{y}\right)^{\alpha/2}\right]}{\alpha(x-y)}\right\} \quad (\alpha < 2), \tag{35}$$

where $\mathfrak{A} = \frac{1}{4\Gamma(-\alpha/2)\Gamma(\alpha/2)\cos^2(\frac{\pi\alpha}{4})}$. Unfortunately, the exact solutions of the eigenvalues and the corresponding eigenfunctions for Eq. (35) are not known and remain an open problem. It is nonetheless both possible and interesting to investigate the properties of the E and ψ, for LRHO problem, numerically. In the next section, we will discuss our numerical findings.

It is worth mentioning that, Eq. (35) is only true for an infinitely large system compared to the subsystem size. However, one can also study LRHO problem in the presence of a boundary but since the boundary of the finite system breaks the translational invariance, we have not been able to find $\Gamma^{\pm 1}$ explicitly because we are not allowed to use a Fourier transform for the finite systems. Therefore we studied this case just numerically, and we will present the results in the next sections. As explained above, we can find the eigenvalues E and the corresponding eigenvectors $\psi(x)$ for a given matrix K, and we can also study the scaling behaviors of the entanglement entropy S and the Rényi entropy S_n.

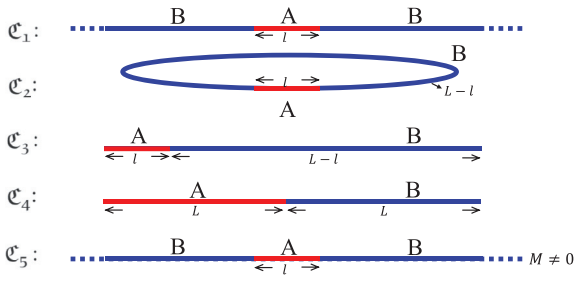

FIG. 1. (Color online) Different configurations of systems and subsystems.

In the next section, we will speak more about our results but here we will discuss different configurations for the system and also subsystem that we used in our study. In this work, we consider five main kinds of configurations depicted in Fig. 1 for a system and a subsystem. In the massless case:

$\mathfrak{C}_1$: The system is very large, and A is a small subsystem with length l.

$\mathfrak{C}_2$: The system with periodic boundary condition has finite size L, and A is a subsystem with length l.

$\mathfrak{C}_3$: The system with size L has boundary and is divided to two adjacent parts. The first part is a subsystem with length $l < L$ and the second part is the complement with size $L - l$.

$\mathfrak{C}_4$: The system with size $2L$ has boundary and is divided to two adjacent equal intervals with length $l = L$ where one of them is the subsystem.

In the massive case:

$\mathfrak{C}_5$: The system is very large, and A is a subsystem with length l.

B. Numerical evaluation

We now numerically evaluate the von Neumann entanglement entropy S and the Rényi entropy S_n for LRHO problem in different cases ($\mathfrak{C}_i, i = 1, \ldots, 5$), by using Eqs. (18) and (21), or equivalently, Eqs. (26) and (27), which was first studied in Ref. 24. In this respect, we follow the method explained in the last section. We will measure the eigenvalues E_i and the eigenfunctions $\psi_i(x)$ in Eq. (23) numerically, and then we will introduce an expression for E and ψ, which matches to the numerical simulations. Our motivation to study these quantities with full detail is related to our interest in better understanding the operator (35), whose eigenvalues provide the entanglement entropy. We should here stress that we calculate the entanglement entropy using the numerical Λ matrix and not by discretizing operator (35). However, we will confirm that these two operators are very close to each other if we consider large systems and consequently can approximate each other.

In order to calculate E and ψ, we first need to construct the matrix Λ for a given K matrix. Numerically, one can

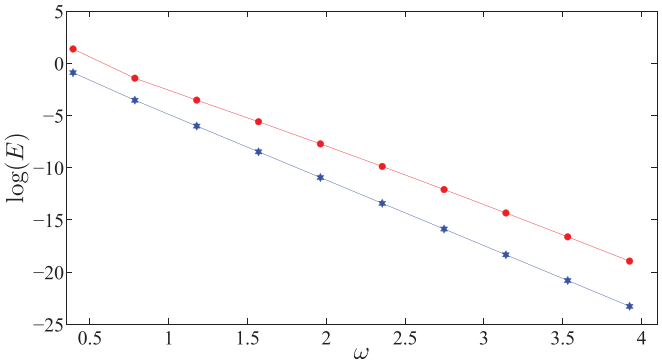

FIG. 2. (Color online) Eigenvalues $\log(E_i)$ vs ω_i for HO with short-range interaction with the configuration $\mathfrak{C}_4$. The blue stars correspond to $E = 1/\sinh(\pi\omega)^2$, where $\omega = n\pi/\log(L)$.

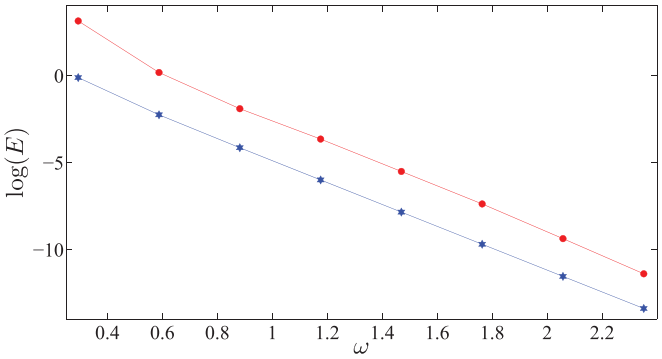

FIG. 3. (Color online) Eigenvalues $\log(E_i)$ vs ω_i for HO with short-range interactions with the configuration $\mathfrak{C}_1$. The blue stars correspond to $E = 1/\sinh(\pi\omega)^2$, where $\omega = n\pi/2[\log(l) + \zeta]$ and $\zeta = 1.3$.

find the matrix $\Lambda \equiv -\Gamma_{+-}^{-1}\Gamma_{-+}$ by multiplying Γ^{-1} and Γ, where $\Gamma = K^{1/2}$ and $\Gamma^{-1} = K^{-1/2}$. For example, we applied this method to the LRHO with a very large system size and small subregion l. There is a very good agreement between numerical Λ and the matrix $\Lambda(x,y)$ coming from Eqs. (33) and (35), when the distances are more than four lattice sizes.

To obtain a better understanding of the long-range harmonic oscillator problem, we studied first the eigenvalues E_i and the eigenfunctions ψ_i of the short-range harmonic oscillator. We considered a system with size $2L$ and the subsystem is taken to be half of the system size ($\mathfrak{C}_4$). Then, using the numerical methods, we diagonalized the matrix Λ to find E_i and ψ_i. In Fig. 2, we sketched a logarithm of the eigenvalues E_i with respect to $\omega(E_i)$. As can be seen, the result obtained from Eq. (29) has similar asymptotic behavior as numerical simulations. In addition, the eigenvectors $\psi(x)$ for the first and second largest eigenvalues, E_1 and E_2 verify the behavior predicted in Eq. (30). We have also calculated the prefactor c numerically and our result is consistent with the theoretical prediction. The numerical results of entanglement entropy for LRHO ($\alpha < 2$) for the systems with boundary, e.g., $\mathfrak{C}_3$ and $\mathfrak{C}_4$, are summarized in the next sections.

Next we discuss the case where the subsystem is very small with length l and the system is very large ($\mathfrak{C}_1$). For this configuration, as a first step, we have studied the properties of E_i and ψ_i for the harmonic oscillator problem with short-range interaction by a direct diagonalization of the matrix Λ. Numerical results are shown in Fig. 3. It is interesting to note that, when we choose $\omega(E_i) = \pi i/2[\log(l) + \zeta]$ ($\zeta = 1.3$), apart from a constant, which appears ubiquitously in this kind of studies[10], the behavior of the eigenvalues E_i is in very good agreement with $E(\omega) = 1/\sinh^2(\pi\omega)$ (see Fig. 2). Let us remark that $\omega(E)$ for the configuration $\mathfrak{C}_1$, differs from Ref. 9 by a factor two and a constant ζ. We studied the scaling of S versus the logarithm of the subsystem size, $\log l$, and compared with Eq. (10). Our result agrees with $c = 1$.

The next step is to analyze the eigenvalues E of the Eq. (35) for LRHO with $\alpha < 2$. As we remarked before, if we consider very small subregion of LRHO with $\alpha = 2$ and very large system size ($\mathfrak{C}_1$), we expect $E_i \sim \sinh^{-2}(\pi\omega_i)$ and $\omega(E_i) = i\pi/2[\log(l) + \zeta]$. For other values of α, the eigenvalues behavior can be seen in Fig. 4, where we compared $\log(E)$ versus ω for various α's. Let us first address the behavior of small eigenvalues E_i (large i, i.e., $i > 3$). Our results show that the small eigenvalues are independent of α, and $\log(E_i)$ is linearly dependent to ω_i by a scaling factor -2π. Then, one can get the asymptotic behavior $E_i \propto e^{-2\pi\omega_i}$ for $i > 3$ and from our previous knowledge about E_i for $\alpha = 2$, one can conjecture the simple behavior $E_i \propto \sinh^{-2}(\pi\omega_i)$. In our numerical simulations, we used $\omega_i = i\pi/2[\log(l) + \zeta]$, where ζ is an α-dependent parameter ($\zeta \in [1.0,2.0]$), to get the best fit to numerical data. We may use this behavior and guess the asymptotic expression for the eigenvalue E as

$$E(\omega) = \frac{a(\alpha)}{\sinh^2(\pi\omega) + b(\alpha)}. \tag{36}$$

The best fit parameters to our numerical data were $a(\alpha) = \frac{\alpha}{2}\sin^2(\frac{\pi\alpha}{4})$ and $b(\alpha) = 0.12\alpha + 0.19\alpha^2 - 0.20\alpha^3 + 0.04\alpha^4$. The value of $b(\alpha)$ is zero at $\alpha = 0$ and 2 and it has a maximum at $\alpha = 1$.

Next, we studied the eigenvector $\psi_i(x)$ of the matrix Λ for LRHO numerically. By diagonalizing Λ, we can also find the eigenvalues E_i. The eigenvector ψ_i can then be computed for each E_i by $\Lambda\psi_i = E_i\psi_i$. A typical example is shown in Fig. 5 where one can see that the eigenfunctions $\psi_i(x)$ are symmetric around $x = l/2$ for odd i and antisymmetric for even i. We

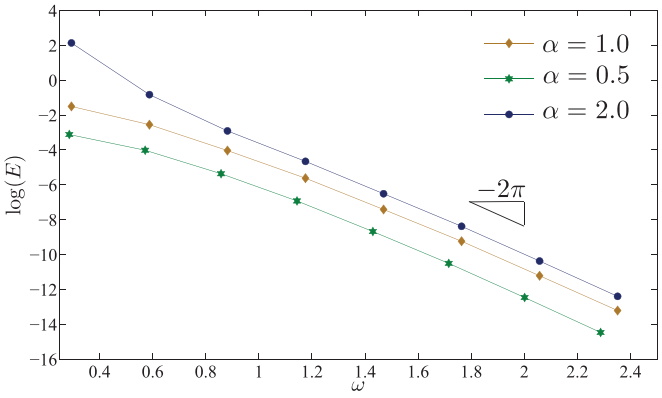

FIG. 4. (Color online) Eigenvalues $\log(E_i)$ vs ω_i for LRHO with the configuration $\mathfrak{C}_1$ and different α's. The small eigenvalues (large ω_i) are independent of α, and $\log(E_i)$ is linearly dependent to ω_i by a scaling factor -2π.

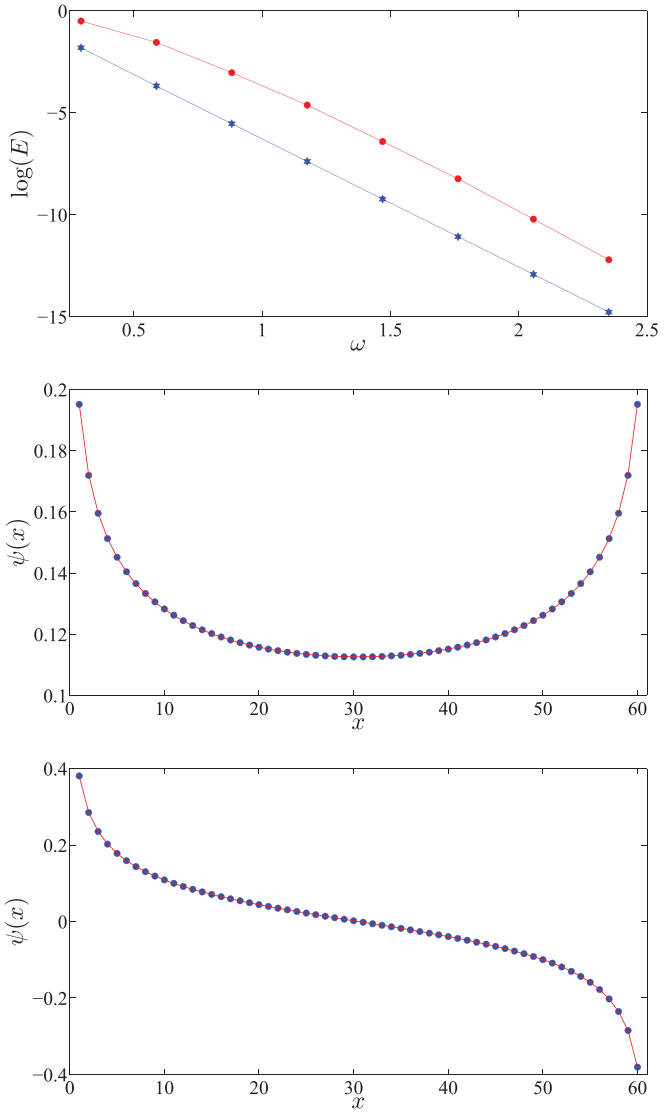

FIG. 5. (Color online) (Top) Eigenvalues $\log(E_i)$ vs ω_i for LRHO ($\alpha = 1$) with the configuration $\mathfrak{C}_1$. The blue stars correspond to $E = \frac{a(1)}{\sinh^2(\pi\omega)+b(1)}$, where $\omega = n\pi/2[\log(l)+\zeta]$ ($\zeta = 1.26$) and $a(1) = 0.25$ and also $b(1) = 0.14$. (Middle) The eigenfunction $\psi_1(x)$ corresponds to the first eigenvalue E_1. (Bottom) The eigenfunction $\psi_2(x)$ corresponds to E_2. Solid red lines correspond to the normalized form of Eq. (37) ($b = -0.26$ and -0.34 for $n = 1$ and 2, respectively).

found that the best fit to the eigenvectors $\psi_i(x)$ is

$$\psi_i(x) = \frac{1}{\mathcal{N}}\{(x^{\imath\omega_i+b} + x^{-\imath\omega_i+b}) - (-1)^i[(l-x)^{\imath\omega_i+b} + (l-x)^{-\imath\omega_i+b}]\}, \quad (37)$$

where $\mathcal{N}$ is the normalization coefficient and $b \in [-1,0]$ is the free parameter to get the best fit to the numerical data. In Eq. (37), we used $\omega_i = \frac{i\pi}{2(\log l+\zeta)}$. The values of the free parameters b and ζ, in general, depend on α. In Fig. 5, the behavior of the ψ for LRHO problem with $\alpha = 1$ and the best fit to Eq. (37) are shown as a function of x.

As argued before, we studied the eigenvalue problem (23) for LRHO, in order to find the eigenfunction $\psi_i(x)$ and the corresponding eigenvalue E_i. The von Neumann entanglement entropy S and the Rényi entropy S_n can be obtained as functions of E [see Eq. (21)]. It is possible to find S and also S_n using Eqs. (26) and (27), respectively.

Finally, we discuss the goodness of Eq. (36). For arbitrary values of the long-range interaction α, the von Neumann entanglement entropy S and the Rényi entropy S_n can in practice be obtained by (i) evaluating Eq. (2) numerically for a system with total size L and compute X_A and P_A from K matrix [see Eq. (24)], (ii) diagonalizing C to obtain ν_i, and (iii) evaluating Eqs. (26) and (27), where l is the number of lattice sites in the subsystem A.

We observe that, in the LRHO problem, the entanglement and the Rényi entropies increase logarithmically with the subsystem size as

$$S \sim \frac{\tilde{c}(\alpha)}{3}\log l \quad (38)$$

and

$$S_n \sim \frac{\tilde{c}_n(\alpha)}{3}\log l, \quad (39)$$

respectively. By studying the scaling behavior of S and also S_n versus $\log l$, one can find the scaling parameters $\tilde{c}(\alpha)$ and $\tilde{c}_n(\alpha)$. We display the resulting quantities for different values of α and n, in Fig. 6.

For arbitrary values of α and n, according to Eqs. (31) and (32) and also Eq. (36), one can find the prefactors $\tilde{c}(\alpha)$ and $\tilde{c}_n(\alpha)$. We have depicted the results coming from these formulas in Fig. 6, and we found perfect agreement between our results, confirming the validity of the Eq. (36). There are some comments in order: the fact that the coefficient of the logarithm is an increasing function of α is somehow counter intuitive because we know that for bigger α's, the interaction get weaker by the distance faster than the smaller α's. There are some ways to roughly understand this result: from mathematical point of view, one might argue that the entanglement entropy is actually related to the eigenvalues of the matrix Λ and those eigenvalues are smaller when we take smaller α's. This can be seen easily by looking at Eq. (35). These eigenvalues are also the parameters that appear after mapping the many-body harmonic oscillator to the two-body case in Eq. (16). Stronger couplings between two oscillators leads to bigger E and, consequently, bigger entanglement among them. The fact that after diagonalization, we have smaller E_i's for smaller α's shows that although the interactions between oscillators far from each other is much stronger for smaller α's, that still does not guaranty bigger entanglement entropy. One might understand these phenomena as follows: based on Eq. (2) in the range $0 < \alpha < 2$, one can see that $K(1)$, which is related to the nearest-neighbor interaction, is an increasing function with respect to α but $K(n)$ with $n > 1$ first increases with α and then decreases. It seems like the value of E_i is mostly dependent on the value of the nearest-neighbor interaction and follows the same trend. So although in some range of α's the next nearest-neighbor interaction for bigger α is smaller, the entanglement after considering the nearest-neighbor interaction is bigger. This also explains qualitatively why we get an increasing function of $a(\alpha)$ in Eq. (36). This reasoning is consistent with the area

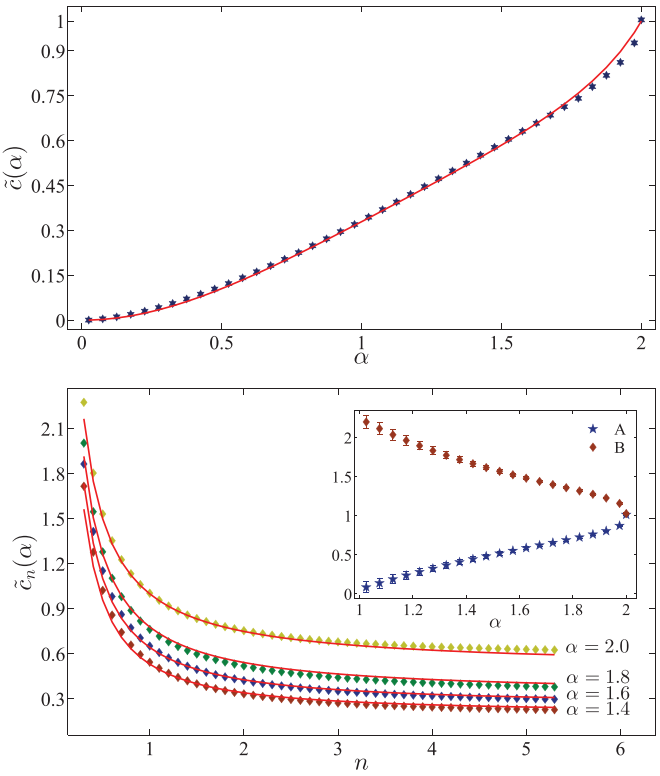

FIG. 6. (Color online) (Top) Prefactor $\tilde{c}(\alpha)$ for discrete system with size $L = 6000$ with the configuration $\mathfrak{C}_1$. The prefactor is measured using the scaling relation S with $\log l$ in the region $0 < l < L/100$. The red line represents the same quantity coming from the continuum limit approximation. (Bottom) $\tilde{c}_n(\alpha)$ vs n for different α's (from top to bottom: $\alpha = 2.0, 1.8, 1.6, 1.4$. The red lines come from the continuum limit approximation. (Inset) A and B coefficients vs α.

law observation in the massive case and also higher dimensions that we are going to discuss later.

We now turn to determine the behavior of $\tilde{c}_n(\alpha)$ with respect to n. Interestingly, we find that the best fit to $\tilde{c}_n$ is

$$\tilde{c}_n(\alpha) = \frac{\tilde{c}(\alpha)}{2}\left[A(\alpha) + \frac{B(\alpha)}{n}\right]. \tag{40}$$

The coefficients $A(\alpha)$ and $B(\alpha)$ are functions of α (see Fig. 6), which indicates that LRHO is not conformally invariant [notice that by definition $A(\alpha) + B(\alpha) = 2$]. In conformal invariant systems, $\tilde{c}_n = \frac{c}{2}(1 + \frac{1}{n})$, where c is the central charge of the system. At this point, it is worth mentioning that one can also calculate the single copy entanglement introduced in Ref. 29. Since this quantity is equivalent to the Rényi entropy with $n \to \infty$, see Ref. 30, we get simply the result $S_\infty = \frac{\tilde{c}(\alpha)}{6} A(\alpha)$, which shows that in this case, in contrast to the short-range case, the single copy entanglement is not just half of the von Neumann entanglement entropy.

In the next section, we will report the results of LRHO in the case of a system that has finite size and also we will report the effect of boundary on the entanglement entropy.

C. Finite-size effects

Until now, to avoid any finite size effect, we concentrated on very large system size $L \to \infty$ and small subsystem size l (configuration $\mathfrak{C}_1$). As mentioned previously, the entanglement entropy S and the Rényi entropy S_n, scale logarithmically with the size of the subregion l ($l \ll L$). However, from the numerical computation of $\tilde{c}_n(\alpha)$, we argued that the LRHO is not conformally invariant except at $\alpha = 2$.

We shall now present a computation of the entanglement entropy for systems with finite size. Conformal field theory predicts[44] the following formulas for the Rényi entropy and the von Neumann entropy of conformally invariant systems with periodic BC's:

$$S^{\mathrm{CFT}}(L,l) = \frac{c}{3}\log\left[\frac{L}{\pi}\sin\left(\frac{\pi l}{L}\right)\right] + c', \tag{41}$$

$$S_n^{\mathrm{CFT}}(L,l) = \frac{c}{6}\left(1 + \frac{1}{n}\right)\log\left[\frac{L}{\pi}\sin\left(\frac{\pi l}{L}\right)\right] + c_n', \tag{42}$$

where c is the central charge and c' and c_n' are nonuniversal constants. Note that Eqs. (41) and (42) are symmetric under $l \to L - l$ and they are maximal when $l = L/2$. For infinite system size, $L \to \infty$ and also the finite one with the condition $l \ll L$, the entanglement entropy scales like Eq. (10).[31] Notice that Eqs. (41) and (42) are only true for conformally invariant systems, and we expect different function in our system.

Here, we will discuss the effect of boundary on the entanglement and Rényi entropies of the LRHO problem. We are interested to study the case in which we take a finite system with half of it as the subsystem. We considered a system with total size $2L$, and the subsystem size L ($\mathfrak{C}_4$). The important subtlety here is the definition of the K matrix. Since we have a finite system, the fractional Laplacian can not be easily defined by its Fourier transform (for more details see Ref. 26). One way to define the fractional Laplacian is based on nonlocal integrals in bounded domain.[34] Although this approach is precise, it is difficult to use it in discrete level for numerical evaluations. We will follow the simpler path, the so-called absorbing boundary condition considered in Ref. 26.

The main difference between K matrix in the finite system with boundary and the infinite one, defined in Ref. 26, is that the K matrix for the system with boundary is defined by throwing away the elements of the infinite matrix that are in the region outside the system.

Let us now consider the Λ matrix and its eigenvalues E for the configuration $\mathfrak{C}_4$. For the short-range interaction problem ($\alpha = 2.0$), the eigenvalues are described by $E = \sinh^{-2}(\pi\omega)$ with $\omega = n\pi/\log(L)$ [see Eq. (29)]. Our calculations for other cases $\alpha < 2$ show that the small eigenvalues are independent of α (see Fig. 7). We found that $E = a(\alpha)/[\sinh^2(\pi\omega) + b(\alpha)]$ [see also Eq. (36)] is a good approximation for the eigenvalues of Λ with $a(\alpha) = \frac{\alpha}{2}\sin^2(\frac{\pi\alpha}{4})$ and $b(\alpha) = 0.32\alpha - 0.08\alpha^2 - 0.16\alpha^3 + 0.06\alpha^4$ as the best numerical fit parameters to our data. The parameter $b(\alpha)$ for the configuration $\mathfrak{C}_4$ differs from the same quantity for the configuration $\mathfrak{C}_1$ except at $\alpha = 2$.

Numerical measurement shows that the entanglement entropy S and the Rényi entropy S_n follow $S \sim \frac{\tilde{c}_4^F(\alpha)}{6}\log L$ and $S_n \sim \frac{\tilde{c}_{4n}^F(\alpha)}{6}\log L$, respectively, where the index 4 indicates

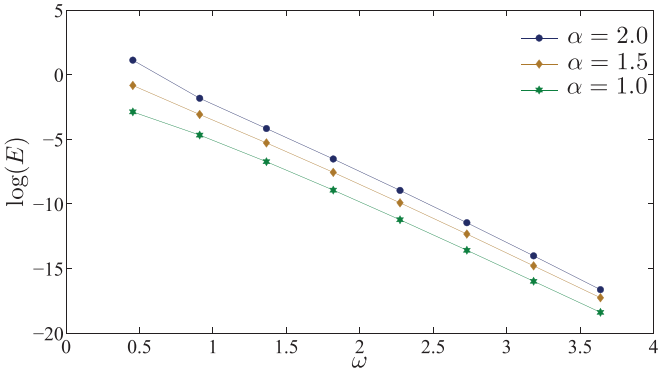

FIG. 7. (Color online) Eigenvalues $\log(E_i)$ vs ω_i for LRHO with the configuration $\mathfrak{C}_4$ and different αs. The small eigenvalues (large ω_i) are independent of α and also $\log(E_i)$ is linearly dependent to ω_i.

the case that we study. In Fig. 8, we report the numerically calculated values $\tilde{c}_4^F(\alpha)$ and $\tilde{c}_{4n}^F(\alpha)$ for several values of α and n.

These prefactors are generally different from $\tilde{c}(\alpha)$ and $\tilde{c}_n(\alpha)$ except at the point $\alpha = 2$. Finally, we found that $\tilde{c}_{4n}^F(\alpha) = \frac{\tilde{c}_4^F(\alpha)}{6}[A^F(\alpha) + B^F(\alpha)/n]$ is the best fit to $\tilde{c}_{4n}^F(\alpha)$ with respect to n [notice that by definition $A^F(\alpha) + B^F(\alpha) = 2$]. The coefficients A^F and also B^F are functions of α (see Fig. 8).

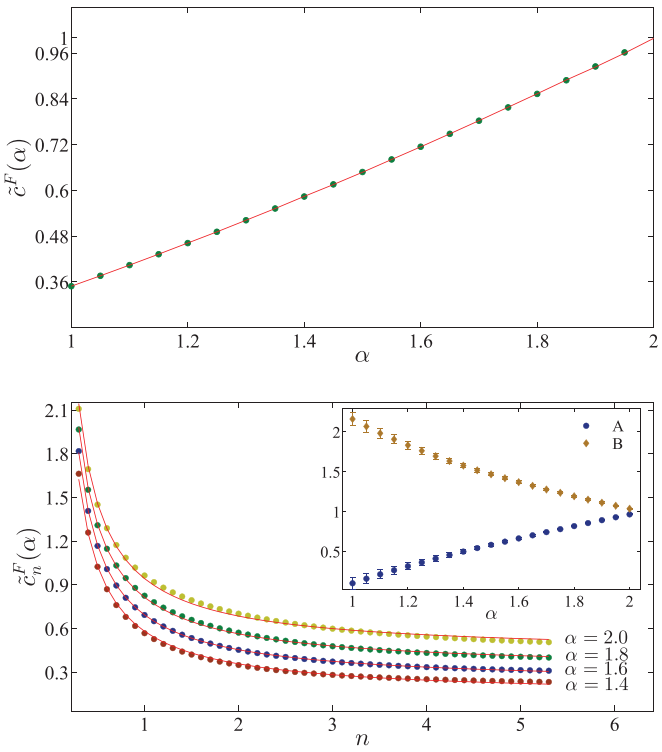

FIG. 8. (Color online) (Top) Scaling prefactor $\tilde{c}_4^F(\alpha)$ for discrete system with configuration $\mathfrak{C}_4$. The red line represents the same quantity coming from the continuum limit approximation. (Bottom) $\tilde{c}_{4n}^4(\alpha)$ for the system with the configuration $\mathfrak{C}_4$ vs n for different α's (from top to bottom: $\alpha = 2.0, 1.8, 1.6, 1.4$). The red lines are the best fit with $\tilde{c}_{4n}^F(\alpha) = \frac{\tilde{c}_4^F(\alpha)}{2}[A^F(\alpha) + B^F(\alpha)/n]$. (Inset) A^F and B^F coefficients vs α.

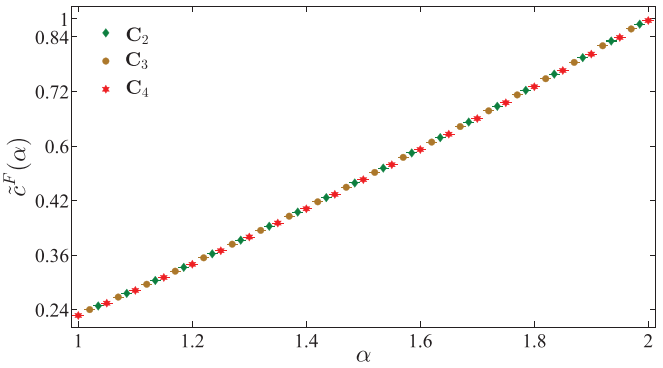

FIG. 9. (Color online) Scaling prefactor $\tilde{c}_i^F(\alpha)$ for discrete systems with configurations $\mathfrak{C}_2$, $\mathfrak{C}_3$, and $\mathfrak{C}_4$.

One can do the same calculations also for the configurations $\mathfrak{C}_2$ (in this case, we considered $l = L/2$ and $S \sim \frac{\tilde{c}_2^F(\alpha)}{3}\log L$) and $\mathfrak{C}_3$ (where we take $S \sim \frac{\tilde{c}_3^F(\alpha)}{6}\log L$). In Fig. 9, we sketched $\tilde{c}^F(\alpha)$. It is clear that the results for different configurations $\mathfrak{C}_2$, $\mathfrak{C}_3$, and $\mathfrak{C}_4$ are similar. In other words,

$$c^F(\alpha) = c_2^F(\alpha) = c_3^F(\alpha) = c_4^F(\alpha). \tag{43}$$

In the next section, we will discus this similarity and we will show that these results are also the same as the massive systems. In case $\mathfrak{C}_3$, to have an idea about the function that controls the finite size effect, we first realized that one can fit the data to the following function:

$$S = \frac{c_3^F(\alpha)}{6}\log\left[L f_{3\alpha}\left(\frac{l}{L}\right)\right], \tag{44}$$

where $f_\alpha(x \to 0) \sim x$ and $f_\alpha(\frac{1}{2}) \sim 1$. One can determine the function f_α by using the formula

$$f_{3\alpha}\left(\frac{l}{L}\right) = e^{\frac{6}{c_3^F(\alpha)}[S_\alpha(l) - S_\alpha(\frac{L}{2})]}. \tag{45}$$

As one can see in Fig. 10, the function is smoothly α dependent. At the same Fig. 10, we also depicted the same function for the case $\mathfrak{C}_2$ where we define $f_{2\alpha}(\frac{l}{L}) = e^{\frac{3}{c_2^F(\alpha)}[S_\alpha(l) - S_\alpha(\frac{L}{2})]}$. It seems that except at the $\alpha = 2$, the forms of the functions are different in two different configurations.

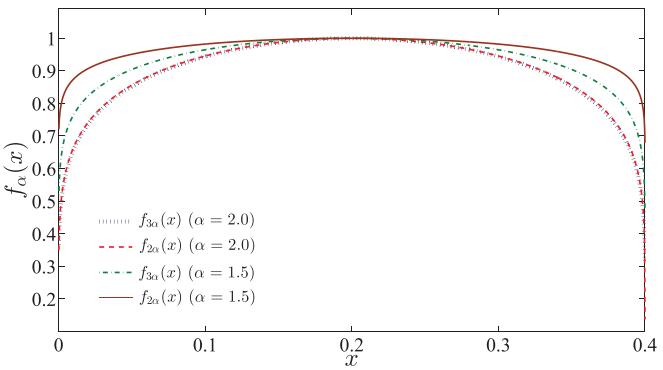

FIG. 10. (Color online) Function $f_\alpha(x)$ $(x = \frac{l}{L})$ for systems with configurations $\mathfrak{C}_2$ and $\mathfrak{C}_3$.

D. Massive LRHO

As noted before, the entanglement entropy S and the Rényi entropy S_n, in massless LRHO (for all configurations $\mathfrak{C}_1$, $\mathfrak{C}_2$, $\mathfrak{C}_3$, and $\mathfrak{C}_4$), increases logarithmically with the subsystem size. We also calculated the prefactors of the logarithms, $\tilde{c}(\alpha)$ and $\tilde{c}_n(\alpha)$ for the case $\mathfrak{C}_1$ and $\tilde{c}^F(\alpha)$ and $\tilde{c}_n^F(\alpha)$ for other cases, as a function of the long-range parameter α and n. Here, we are interested in characterizing the massive long-range interacting harmonic oscillators.

First, we consider a finite interval of length l in a massive system (configuration $\mathfrak{C}_5$). Following an argument given by Calabrese and Cardy,[31] the entanglement entropy for such a system gets saturated by a mass scale and increases logarithmically $S = -\kappa \frac{c}{6} \log M$, where c is the central charge of the system and it is equal to one for short-range harmonic oscillators and M is the mass of the system. The prefactor κ is the number of boundary points between subsystem A and its complement with $\kappa = 1$ for a system with boundary and $\kappa = 2$ for a system with periodic boundary condition.[4]

We now consider the LRHO problem, Eq. (2) with mass $M > 0$. As discussed before, we are again going to calculate the entropy S numerically. The results clearly show that S saturates in the $l \to \infty$ and the entropy S changes logarithmically with respect to the mass

$$S = -\frac{\tilde{c}^g(\alpha)}{3} \log M. \tag{46}$$

Using such scaling form, we have obtained the prefactor $\tilde{c}^g(\alpha)$, as illustrated in Fig. 11, as a function of α. Surprisingly, we found that the prefactor is the same as the prefactor of the system with periodic boundary condition when we take half of the system (see Fig. 11). We also considered a massive system with boundary and the numerical results perfectly agree with $S = -\frac{\tilde{c}^g(\alpha)}{6} \log M$.

Next, we turn to speak more about the Rényi entropy S_n for the massive case. Our analysis shows that S_n has also logarithmic scaling with the subsystem size and we measured the prefactor $\tilde{c}_n^g(\alpha)$. Interestingly, we found that this exponent is the same as $\tilde{c}_n^F(\alpha)$. This is shown in Fig. 11. To have an understanding of this equality, we note that we generated the K matrix for the system with boundary ($M = 0$) by throwing away those elements of the infinite system that are not inside the corresponding finite system. In this case, the summation of every row of the K matrix is nonzero. This corresponds to an effective mass in the system and the system will be gapped. This effective mass is equivalent to the correlation length $\xi_t = \frac{1}{m^{\alpha/2}}$. Therefore this argument hints that the results of massive LRHO should be similar to the massless one when the system has boundary.

E. Finite temperature

In this section, we present numerical results for the coupled harmonic oscillators with long-range interaction in thermal states. Consider the Hamiltonian $\mathcal{H}$ at some temperature $T > 0$. The Gibbs state corresponding to this temperature, associated with the canonical ensemble, is given by

$$\rho(\beta) = \exp(-\beta\mathcal{H})/\mathrm{tr}[\exp(-\beta\mathcal{H})], \tag{47}$$

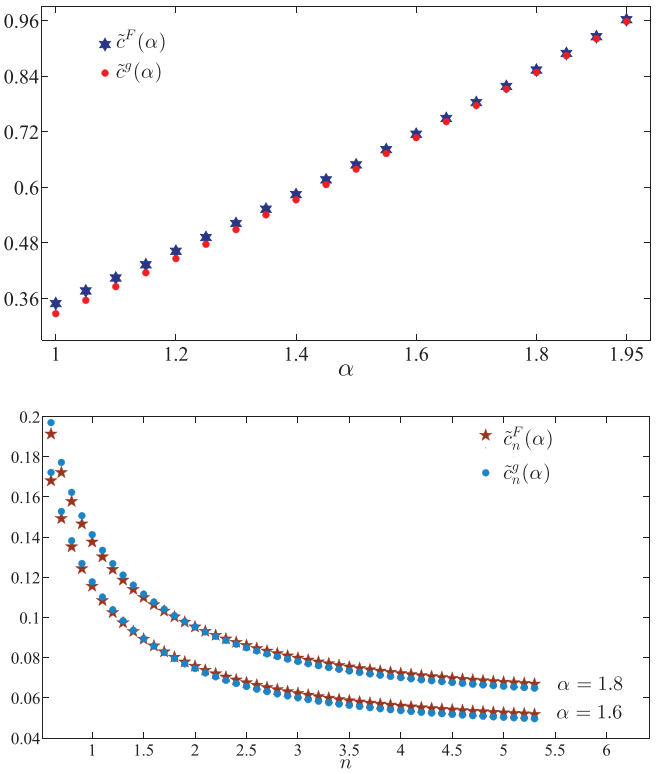

FIG. 11. (Color online) (Top) Prefactor $\tilde{c}^g(\alpha)$ compared with $\tilde{c}^F(\alpha)$ as a function of α. (Bottom) Prefactor $\tilde{c}_n^g(\alpha)$ for massive LRHO with the configuration $\mathfrak{C}_5$ is the same as $\tilde{c}_n^F(\alpha)$ for a massless one with the configurations $\mathfrak{C}_2$, $\mathfrak{C}_3$, and $\mathfrak{C}_4$.

where $\beta = 1/T$. Similar to the zero temperature case, one can obtain the covariance matrix $C(\beta)$ and also two-point correlators $P(\beta)$ and $X(\beta)$ of the state $\rho(\beta)$ in the basis in which the Hamiltonian matrix is diagonal. These matrices are given by[18]

$$P(\beta) = \tfrac{1}{2} K^{1/2} W(T), \quad X(\beta) = \tfrac{1}{2} K^{-1/2} W(T), \tag{48}$$

and

$$C^2(\beta) = \tfrac{1}{4} [K^{-1/2} W(T)] \oplus [K^{1/2} W(T)], \tag{49}$$

where $W(T) := \mathbb{I} + 2[\exp(K^{1/2}/T) - \mathbb{I}]^{-1}$. It is worth mentioning that the entropy of the subsystem with length l at temperature T for CFT is given by the formula[31]

$$S = \frac{c}{3} \log \left(\frac{\beta}{\pi} \sinh \frac{\pi l}{\beta} \right) + c_1'. \tag{50}$$

As expected, in the zero- and high-temperature limits, the von Neumann entropy reduces to $S = \frac{c}{3} \log l + c_1'$ and $S = \frac{\pi c}{3\beta} l + c_1'$, respectively. In the high-temperature limit, the von Neumann entropy has an extensive form and it reduces to the standard CFT and agrees with the Gibbs entropy of an isolated system of length l.[31]

As in previous cases, our aim is to study the properties of the von Neumann entropy of a system of harmonic oscillators with the long-range interaction at finite temperature. For simplicity, we focus on the high-temperature limit. In order to measure the von Neumann entropy, we needed to restrict the system size to the finite values with total size L, and subsystem size $1 \ll l \ll L$, to avoid the finite size problem. In order to calculate the

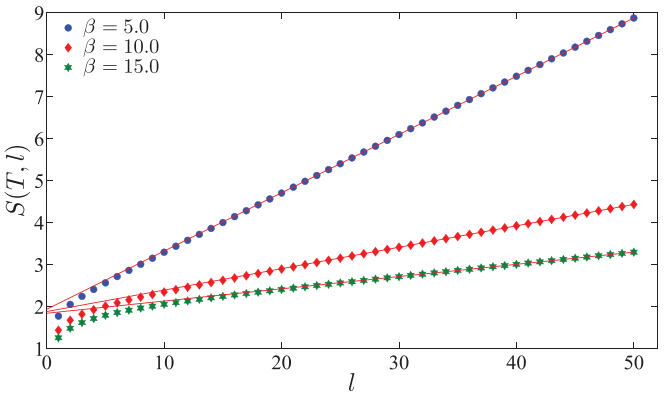

FIG. 12. (Color online) Von Neumann entropy for LRHO ($\alpha = 1.4$) with the system size $L = 5000$, in the finite temperature $T = 1/\beta$.

von Neumann in this state, we need to consider the covariance matrix (49) associated with the reduced state of an interval with length l. Thus we calculated $C(\beta)$ at some particular values $T = 1/\beta$ and then performed the diagonalization of the covariance matrix to find $S(T,l)$.

As shown in Fig. 12, in the high-temperature limit, $S(T,l)$ for various values of T and α is a linear function of l, so in this case, one has

$$S \sim \lambda l T^{\xi}, \tag{51}$$

where λ and ξ are functions of α. The log-log plot S/l with respect to T is shown in Fig. 13. The scaling parameter ξ and the prefactor λ are shown in Fig. 13. The scaling exponent ξ and the quantity $2/\alpha$ are the same, and one can nicely interpolate $\xi = 2/\alpha$. This is not surprising because it is well known that in the long-range systems the dynamical exponent is $z = \frac{\alpha}{2}$, and this exponent controls the relative scaling of time and space leading to the invariant form $lT^{1/z}$.[35] In general, the thermal entropy for the theories with the dynamical exponent $z \neq 1$ scales as $lT^{1/z}$, which follows from the requirement of dimensionlessness and extensivity.[35] Returning to our LRHO problem, we can conclude that the entropy in the high-temperature limit should follow the simple form $S \propto lT^{2/\alpha}$.

It is interesting to note that the Rényi entropy S_n for finite temperature LRHO, in the high-temperature limit is

$$S_n \sim \lambda_n l T^{\xi}. \tag{52}$$

In Fig. 13, we show the prefactor λ_n as a function of n for several α's. It is worth mentioning that all the curves have similar behavior at large n ($\lambda_\infty = \pi/6$).

F. Universality

In the previous sections, we studied a particular case of long-range harmonic oscillator that leads to a well-defined continuum limit field theory. This is a hint to believe that probably the results that we found are robust and valid for larger set of harmonic oscillators. In this section, we would like to address this question by first studying a long-range harmonic oscillator in the presence of a short-range harmonic

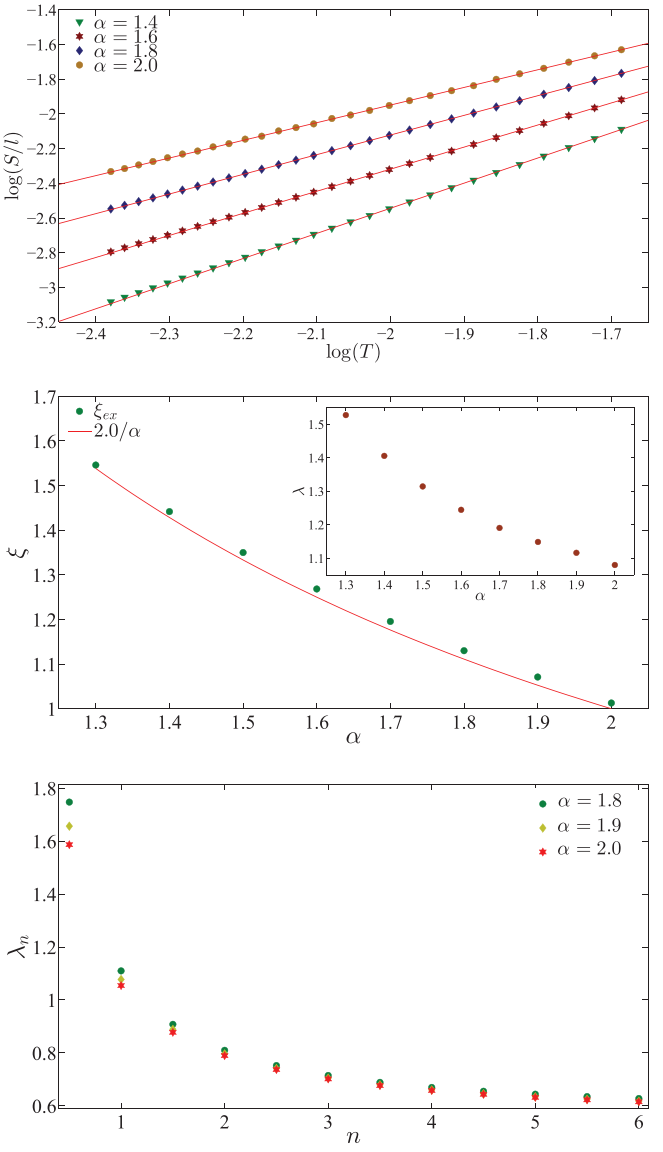

FIG. 13. (Color online) (Top) Entanglement entropy for LRHO with finite temperature shows the scaling behavior $S(T,l)/l \sim \lambda T^{\xi}$, in the high-temperature limit. (Middle) Scaling exponent ξ as a function of α. The solid red line represents $\xi = 2/\alpha$. The parameter λ is shown in the inset. (Bottom) Parameter λ_n for the Rényi entropy of LRHO with finite temperature in the high-temperature limit.

oscillator and then by investigating a larger set of interactions that can be decomposed into our studied systems.

1. Long-range HO in the presence of short-range HO

So far, we have only considered the harmonic oscillator systems with the long-range interaction. In the last section, we studied LRHO by means of the eigenvalue problem and we computed the eigenvalue E and the eigenfunction ψ numerically. In a similar way, we will try to do the same calculation for harmonic oscillator systems with long-range plus short-range interactions. Then, we will study the logarithmic scaling of the entanglement entropy S and also Rényi entropy S_n for this model. Finally, we are going to

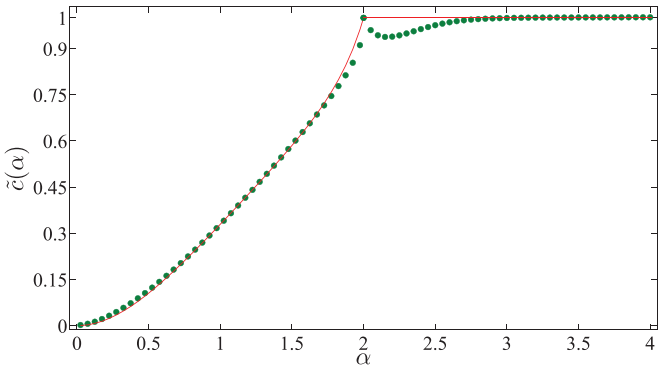

FIG. 14. (Color online) Green (Dark gray) circles represent $\tilde{c}(\alpha)$ for the system of harmonic oscillator with long-range plus short-range interactions with the configuration $\mathfrak{C}_1$. The prefactor $\tilde{c}(\alpha)$ is measured using the scaling relation S with $\log l$ in the region $0 < l < L/100$ for the system size $L = 6000$. The red line represents the same quantity for the pure LRHO.

analyze the scaling coefficient $\tilde{c}(\alpha)$ and $\tilde{c}_n(\alpha)$ as functions of α.

Consider the Hamiltonian (1), with long-range plus short-range interactions:

$$K = K_{\mathrm{LR}} + K_{\mathrm{SR}}, \tag{53}$$

where K_{LR} is again defined as Eq. (2), and K_{SR} is just a simple Laplacian. We have only considered the massless system with $M = 0$ but one can also generalize them to $m \neq 0$.

We have carried out simulations for $0 < \alpha < 4$. For each value of α, we have determined the matrix K for a large enough system size with $L = 6000$ with the subsystem size less than $L/100$. The entanglement entropy grows logarithmically with the subsystem size as $S = \frac{\tilde{c}(\alpha)}{3}\log(l)$, where $\tilde{c}(\alpha)$ is a function of α. We have depicted $\tilde{c}(\alpha)$ versus α in Fig. 14, where the solid line comes from LRHO case. It is also interesting to note the similarity of $\tilde{c}(\alpha)$ in the range $\alpha < 2$ with the results of a harmonic oscillator (HO) with pure long-range interaction and also $\alpha \geqslant 2$ with the result of an HO with pure short-range interaction (see Fig. 14). The entanglement entropy of a harmonic oscillator system with long-range plus shot-range interactions with the exponent $\alpha < 2$ ($\alpha \geqslant 2$) is the same as a harmonic oscillator system with pure long-range (short-range) interaction. This might look not surprising because we know that from the renormalization group point of view the short-range interaction is irrelevant as far as $\alpha < 2$. In our numerical calculation, the reason of discrepancy in the region $2 < \alpha \leqslant 2.5$ is unclear to us.

We also calculated the Rényi entropy S_n for coupled harmonic oscillators with long-range plus short range couplings. To get S_n numerically, we used Eq. (21). We found that for $l \ll L$ the Rényi entropy also logarithmically increases with the system size as $S_n = \frac{\tilde{c}_n(\alpha)}{3}\log(l)$, where the prefactor $\tilde{c}_n(\alpha)$ is a function of n and also α. The best fit is $\tilde{c}_n(\alpha) = \frac{\tilde{c}(\alpha)}{2}[A(\alpha) + B(\alpha)/n]$. The resulting values of $A(\alpha)$ and $B(\alpha)$ as a function of α are represented in Fig. 15. We remark that, for $\alpha < 2$, the data are in excellent agreement with the LRHO,[24] whereas for $\alpha \geqslant 2$ they agree with the short-range prediction. On the other hand, the system is conformally invariant for $\alpha \geqslant 2$ where we have $A = B = 1$.

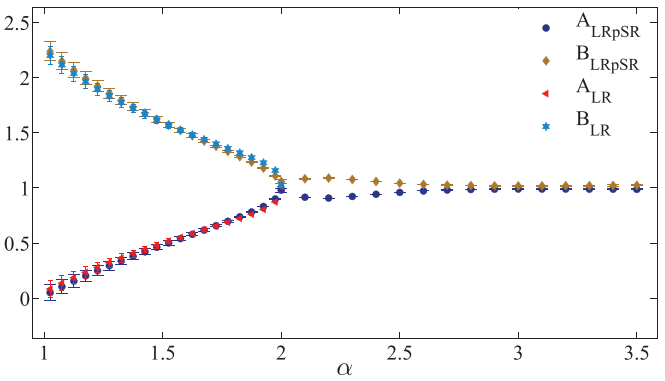

FIG. 15. (Color online) $A(\alpha)$ and $B(\alpha)$ coefficients vs α for system of harmonic oscillator with long-range plus short-range interactions.

We now consider the entanglement entropy of a system of long-range harmonic oscillator with $K = K^{\alpha}_{\mathrm{LR}} + K^{\alpha'}_{\mathrm{LR}}$, where K^{α}_{LR} is defined as in Eq. (2). The entanglement entropy grows logarithmically with the subsystem size and the prefactor is equal to $\tilde{c} \sim \min\{\tilde{c}(\alpha), \tilde{c}(\alpha')\}$. The results of the prefactor $\tilde{c}$ are depicted in Fig. 16. For $\alpha \geqslant \alpha'$, we expect $\tilde{c} \sim \tilde{c}(\alpha')$ but when $\alpha \sim \alpha'$, we observe a large discrepancy in the numerical results.

2. *Generalization to singular Toeplitz matrices*

In this section, we would like to address how one can relate the entanglement entropy of more general harmonic oscillators to the entanglement entropy of the studied long-range harmonic oscillators. Although our conclusion is based on just numerical evaluations we will show in the section dedicated to the mutual information that in some particular cases one can derive the results analytically. We define the Hamiltonian of the harmonic oscillator with the following K matrix:

$$K_{l,m} = -\int_0^{2\pi} \frac{dq}{2\pi} e^{iq(l-m)} b(q) \prod_{r=1}^{R} u(\alpha_r, q - q_r), \tag{54}$$

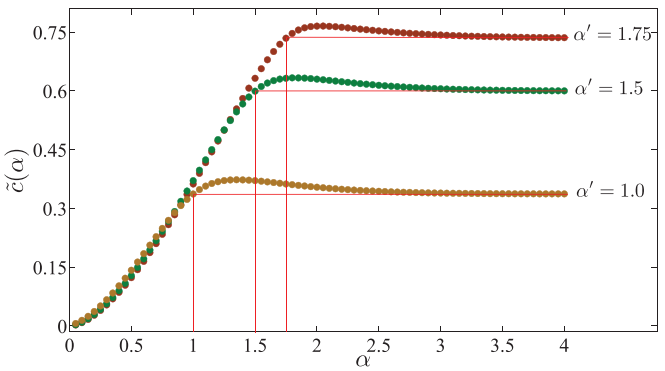

FIG. 16. (Color online) Prefactor $\tilde{c}(\alpha)$ for the system of a harmonic oscillator with a long-range interaction with exponent α plus another long-range interaction with the exponent α'. It seems that $\tilde{c} \sim \min\{\tilde{c}(\alpha), \tilde{c}(\alpha')\}$. The prefactor $\tilde{c}(\alpha)$ is measured using the scaling relation S with $\log l$ in the region $0 < l < L/100$ for the system size $L = 6000$.

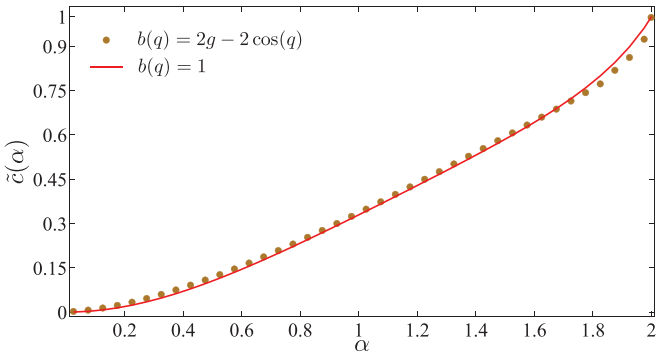

FIG. 17. (Color online) Prefactor of logarithm for the entanglement entropy for nontrivial $b(q)$ function. For $g > 1$, the prefactor is independent of the $b(q)$ function.

where $b(q) : S^1 \to \mathcal{C}$ is a smooth nonvanishing function with zero winding number and

$$u(\alpha,q) = (2 - 2\cos q)^{\frac{\alpha}{2}}. \tag{55}$$

The above Toeplitz matrices are usually called singular Toeplitz matrices. For our purpose, we need to also consider some particular restrictions on q_r to have real interactions between harmonic oscillators. From now on, we will consider just those q_r's that e^{iq_r}'s are either real or the complex conjugate of each other for every α_r. Harmonic oscillators with the above interactions are critical and one can simply show that $\xi^{-1} = 0$. The above interactions are natural generalizations of the ones that we considered in previous sections. One way to see this is by considering $2m - 2\cos q$ instead of $2 - \cos q$ in Eq. (2). For $m = \cos q_r$, one can simply show that $|2m - 2\cos q| = [2 - 2\cos(q + q_r)]^{\frac{1}{2}}[2 - 2\cos(q - q_r)]^{\frac{1}{2}}$, which is in the form of Eq. (54). It is worth mentioning that for $m > 1$ the system is gapped and otherwise it is gapless.

Using the techniques of the previous sections, one can calculate easily the entanglement entropy of these harmonic oscillators. The entanglement entropy changes logarithmically with the subsystem size and the prefactor of the logarithm is a function that is independent of $b(q)$ and q_r but it is strongly dependent on the α_r's. To show that the results are $b(q)$ independent, we took $b(q) = 2g - 2\cos(q)$ with $g > 1$ for several g for $R = 1$. The results are shown in the Figs. 17 and 18 where one can see that the prefactor of the logarithm

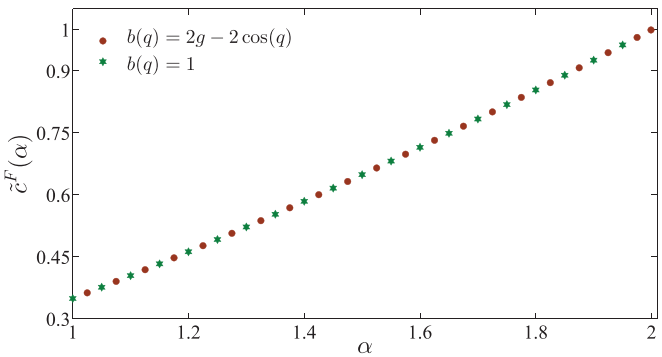

FIG. 18. (Color online) Prefactor of logarithm in the presence of boundary for nontrivial $b(q)$ function. For $g > 2$, the prefactor is independent of the $b(q)$ function.

TABLE I. Numerical values of the prefactor $\tilde{c}$ for different values of α_r and q_r.

q_1	q_2	q_3	q_4	q_5	q_6	α_1	α_2	α_3	α_4	α_5	α_6	$\tilde{c}/2$
$\frac{\pi}{3}$	$\frac{-\pi}{3}$	0	0	0	0	1	1	0	0	0	0	0.33(0.01)
$\frac{\pi}{6}$	$\frac{-\pi}{6}$	0	0	0	0	1	1	0	0	0	0	0.33(0.01)
0	0	$\frac{\pi}{3}$	$\frac{-\pi}{3}$	0	0	0	0	1.5	1.5	0	0	0.60(0.01)
0	0	0	0	$\frac{\pi}{3}$	$\frac{-\pi}{3}$	0	0	0	0	2	2	0.99(0.01)
$\frac{\pi}{3}$	$\frac{-\pi}{3}$	$\frac{\pi}{6}$	$\frac{-\pi}{6}$	0	0	1	1	1.5	1.5	0	0	0.92(0.01)
$\frac{\pi}{3}$	$\frac{-\pi}{3}$	$\frac{\pi}{6}$	$\frac{-\pi}{6}$	0	0	1	1	1.5	1.5	2	2	1.91(0.01)
$\frac{\pi}{3}$	$\frac{-\pi}{3}$	$\frac{\pi}{6}$	$\frac{-\pi}{6}$	$\frac{\pi}{4}$	$\frac{-\pi}{4}$	1	1	1.5	1.5	2	2	1.93(0.01)

is the same in all the different cases. We conjecture that the prefactor of the logarithm is independent of the form of the function $b(q)$. Next, we calculated the prefactor of the logarithm for different values of α_r and q_r. The results are shown in Table I.

It is easy to see that first, the results are independent of q_r's, and second, one can get the results of the last three rows by just summing the results of the first four rows. Based on the results of the table, one can conjecture that for the interaction (54), the following result is valid for the prefactor of the logarithm:

$$\begin{aligned}&\tilde{c}(\alpha_1,\alpha_1,\alpha_3,\alpha_3,\ldots,\alpha_{R-1},\alpha_{R-1})\\ &\quad= \tilde{c}(\alpha_1,\alpha_1,\ldots,0) + \tilde{c}(0,0,\alpha_2,\alpha_2,\ldots,0)\\ &\qquad+\cdots+\tilde{c}(0,0,\ldots,\alpha_{R-1},\alpha_{R-1}).\end{aligned} \tag{56}$$

In other words, one can get the prefactor of the logarithm in the model (54) by just having the same quantities for the long-range harmonic oscillator that we have discussed in the previous sections

G. Two dimensions: area law and logarithmic term for polygonal region

It was shown in Ref. 8 that the area law is valid for short-range harmonic oscillator if we consider a sphere like region in higher dimensions. The coefficient of the area term is a nonuniversal number. For example, if we take a squarelike subregion, then the coefficient of the area term will be dependent to the orientation of the polygon with respect to the symmetry axes of the lattice. Later, it was shown in Ref. 36 that if we consider a region with sharp corners, then in the entanglement entropy there will be also some extra logarithmic terms with universal coefficients. In other words, one can write the entanglement entropy of a polygon as

$$S(\theta) = a_0 + a_1 L + a_{-1}L^{-1} + a_{-2}L^{-2} - s(\theta,\alpha)\log L, \tag{57}$$

where L is the size of the system and θ is the vertex angle of the polygon. Following the same procedure as in previous sections, we first found the entanglement entropy of the squarelike regions for different values of α's and confirmed that the leading term is the area law. The coefficient a_1 was an increasing function of α [see Fig. 19). Using Eq. (57), we found $s(\theta,\alpha)$ for different values of θ, $\theta = \frac{\pi}{4}, \frac{\pi}{2}, \frac{3\pi}{4}$, and different values of α. The results are depicted in Fig. 19. We also showed that the coefficients $s(\theta,\alpha)$ are independent of the orientation of the subregion with respect to the symmetry axes of the lattice. One can summarize this section as follows:

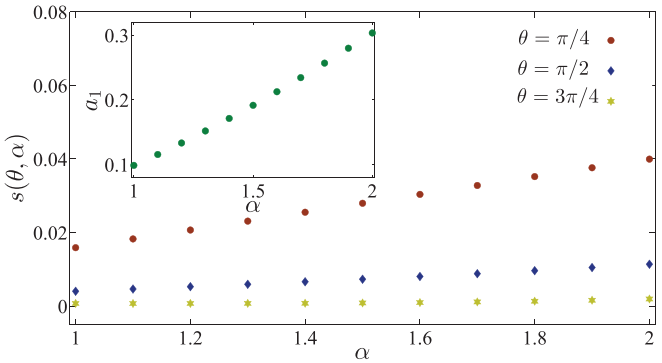

FIG. 19. (Color online) $s(\theta,\alpha)$ as a function of α for subsystems with different vertex angles θ. (Inset) Nonuniversal coefficient of the area term a_1 with respect to different values of α.

the entanglement entropy of a polygonal region for long-range harmonic oscillators follows the same formula as the short-range one but with different coefficients. We also confirmed that the same kind of behavior is also valid for Rényi entropy.

IV. MUTUAL INFORMATION

In the previous sections, we studied the von Neumann entropy S and the Rényi entropy S_n for long-range harmonic oscillators with different configurations of systems and subsystems. It is also of considerable interest to quantify the Shannon's classical mutual information[37] for a system of harmonic oscillators with short- and long-range interactions. The Shannon information for spin systems was first studied in Ref. 38 and much more investigated in Refs. 39–42 for different quantum systems. Here, we focus to the definitions given in Refs. 18, 27, and 42.

Consider a chain of L harmonic oscillators described by canonical variables (ϕ_i,π_i), $i = 1,2,\ldots,L$, and the system is divided in two parts A and B with l and $L-l$ oscillators, respectively. The oscillators are coupled by a quadratic Hamiltonian (1). Let us now consider $\Phi_A = (\phi_1,\phi_2,\ldots,\phi_l)$ and $\Phi_B = (\phi_{l+1},\phi_{l+2},\ldots,\phi_L)$ the position vectors of the subsystems A and B and $\Pi_{A,B}$ the respective momentum vectors. The classical mutual information can be defined as

$$I(A,b) = S_A + S_B - S_{(A+B)}, \tag{58}$$

where S is the Shannon's classical entropy. There are in fact two different definitions to evaluate Shannon's mutual information. The difference comes from the source of probabilities that we use to define the entropy. In the first case, we use the ground state of the quantum system as the source of the probabilities for appearing different configurations and in the second case it will be just the Gibbs distribution. The first definition, which has recently found many interesting applications in the study of spin chains,[38,40–42] can be defined in the context of harmonic oscillators as follows: the Shannon's classical mutual information $I(A:B)$ between two regions A and B is

$$I_1(A:B) = \int d^N\Phi p(\Phi_A,\Phi_B)\ln\frac{p(\Phi_A,\Phi_B)}{p(\Phi_A)p(\Phi_B)}, \tag{59}$$

where $p(\Phi_A,\Phi_B) = |\Psi_0|^2$ is the total and $p(\Phi_A) = \int[\prod_{m\in(B)} d\phi_m]|\Psi_0|^2$ and $p(\Phi_B) = \int[\prod_{m\in(A)} d\phi_m]|\Psi_0|^2$ are the reduced probability densities in position space [Ψ_0 is the ground-state wave function, i.e., Eq. (12)].[27]

The mutual information $I(A:B)$ or $I(A:B)$ quantifies how correlated the two parts are when the system is in the ground state and for harmonic oscillators has the following simple form:

$$\begin{aligned} I_1(A:B) &= \frac{1}{2}\ln\frac{(\det 2X_A)(\det 2X_B)}{\det K^{-1/2}} \\ &= \frac{1}{2}\ln\frac{(\det 2P_A)(\det 2P_B)}{\det K^{1/2}} \\ &= \frac{1}{2}\ln(\det 4X_A P_A) = \sum_{i=1}^{l}\ln 2\nu_i, \end{aligned} \tag{60}$$

where X_A and P_A are l-dimensional matrices describing correlations within a compact block of l oscillators (subsystem A) and ν_i is the eigenvalue of the matrix $C = \sqrt{X_A P_A}$ and X_B and P_B are $(L-l)\times(L-l)$ matrices describing correlations within subsystem B, and the matrices X_{AB} and P_{AB} describe the correlations between them [see Eq. (24)].[27] It is worth mentioning that the mutual information I_1 is the *lower bound* to the quantum entanglement entropy S.[27] Note that Shannon's mutual information I_1 [see Eq. (60)] is equal to the Rényi entropy S_n [see Eq. (27)] when $n = 2$.[42]

According to Eqs. (2) and (3), K and $K^{\pm 1/2}$ matrices, for a translational invariant system, are Toeplitz matrices. Therefore, to compute the Shannon's classical mutual information Eq. (59), we need to compute the Teoplitz determinants. As shown by Fisher-Hartwig and proved later by Widom[43] (see Appendix), the asymptotic behavior of the Toeplitz determinants $\det(P_A)$ for the massless system, i.e., Eq. (3), with subsystem size $l \gg 1$ is

$$\det P_A \propto l^{\alpha^2/16}. \tag{61}$$

It is also possible to apply the Fisher-Hartwig theorem to X_A when $\alpha < 2$. Then one can find the power-law behavior

$$\det X_A \propto l^{\alpha^2/16}. \tag{62}$$

We have numerically calculated X_A for $\alpha = 2$ and found an agreement with Eq. (62).

Equations (61) and (62) provide an explicit way to find the logarithmic behavior of the mutual information I_1 in terms of the system size. In the case where the system is very large and the subsystem has small size l, the mutual information I_1 can be obtained:

$$I_1 = \frac{\alpha^2}{16}\ln l + c_0. \tag{63}$$

Numerical simulation results (see Fig. 20), in a wide range of α, are in good agreement with Eq. (63), but when $1.5 < \alpha < 2$, we observe small discrepancy in the numerical results. The reason of this discrepancy is unclear to us.

Here, we also focus on the other definition considered by Cramer *et al.*[18] to evaluate Shannon's mutual information. They determined the classical Shannon entropy of the total lattice $S_{(A+B)}$, as well as the entropy S_A and S_B determined by the reduced densities describing the two regions A and

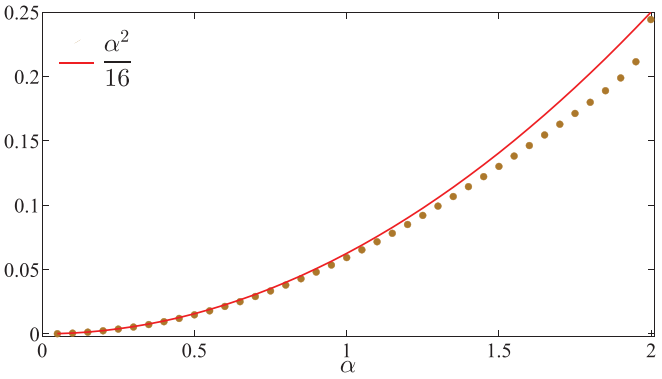

FIG. 20. (Color online) Prefactor of the logarithmic scaling of the mutual information I_1 for LRHO with configuration $\mathfrak{C}_1$.

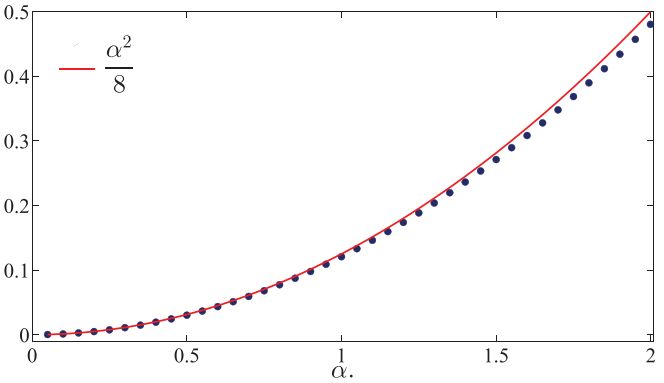

FIG. 21. (Color online) Prefactor of the logarithmic scaling of the mutual information I_2 for LRHO with configuration $\mathfrak{C}_1$.

B, respectively. The classical Shannon entropy for harmonic oscillator at finite temperature $T = 1/\beta$ is

$$S_{\oplus} = -\frac{1}{2}\ln\det(K|_{\oplus})^{-1} + v(\oplus)\ln\frac{2\pi}{\beta} + v(\oplus), \quad (64)$$

where $\oplus \in \{A, B, (A+B)\}$ and $K|_{\oplus}$ denotes the K matrix associated with the corresponding region $\oplus$ and v is the size of the region. Then for a Hamiltonian of the form (1), one can compute the Shannon's mutual information by the following formula:

$$I_2 = \frac{1}{2}\ln\frac{(\det K|_A)(\det K|_B)}{\det K} = \frac{1}{2}\ln(\det K|_A K^{-1}|_A), \quad (65)$$

where $K^{-1}|_A$ denotes the K^{-1} matrix associated with the interior region A. It is worth mentioning that the mutual information I_2 is independent of temperature.

Using Fisher-Hartwig theorem, one can get the asymptotic behavior of the Toeplitz determinants $\det(K|_A)$ for the massless system, i.e., Eq. (2) as

$$\det K|_A \propto l^{\alpha^2/4}. \quad (66)$$

We will now discuss our numerical calculations. First, suppose a very large system and a very small subsystem size (configuration $\mathfrak{C}_1$). In order to compute the mutual information, we have numerically calculated the $K|_A$ and $K^{-1}|_A$ matrices. Then we calculated the eigenvalues of the matrix product $K|_A K^{-1}|_A$ and we measured the mutual information I_2 by the Eq. (65). Our results show the mutual information for LRHO increases logarithmically with the subsystem size as

$$I_2 = \frac{\alpha^2}{8}\ln l + c_0. \quad (67)$$

We then measured the prefactor of the logarithm and our results are shown in the Fig. 21. As we shall discuss in the next sections, it is easy to extend our numerical computation to general configurations of systems and subsystems, i.e., the configurations $\mathfrak{C}_2$, $\mathfrak{C}_3$, and $\mathfrak{C}_4$.

A. Finite systems

Here, we focus on the effect of the finite size system on the mutual information. Hence we shall first consider the mutual information I_1. Consider the case when the system has size L and the subsystem has size $l = L/2$ (configuration $\mathfrak{C}_2$ and $\mathfrak{C}_4$). The mutual information I_1 for systems with size L and subsystem size $l = L/2$ with periodic boundary condition (configuration $\mathfrak{C}_2$) follows:[27]

$$I_1 = \frac{\alpha^2}{16}\ln L + c_0, \quad (68)$$

where α is the scaling exponent for the LRHO, L is the size of the system, and c_0 is the nonuniversal constant.[27]

Then consider the case with configuration $\mathfrak{C}_4$. In this case, the mutual information I_1 follows:

$$I_1 = \frac{\alpha^2}{32}\ln L + c_0. \quad (69)$$

The numerical results of the prefactor of the logarithmic scaling Eqs. (68) and (69) for various α's are displayed in Fig. 22. The agreement between the theoretical results given by Eqs. (68) and (69) and the numerical results is fairly good.

Now we are interested to find the mutual information I_2 for systems with finite size. First, consider configuration $\mathfrak{C}_2$, when the subsystem has size $1 < l < L/2$ and the system has periodic boundary condition. Finite size effects bend down the mutual information when the size of the subsystem approaches half of the system size.

Recall from Eq. (66) that $\det K|_A \propto l^{\alpha^2/4}$ and $\det K|_B \propto (L-l)^{\alpha^2/4}$ for a subsystem of length l in a finite system of

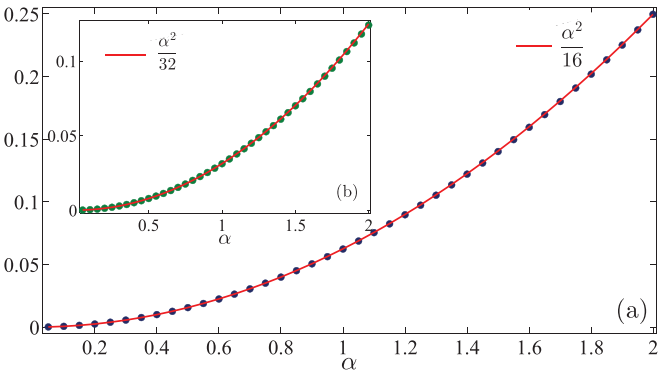

FIG. 22. (Color online) Prefactor of the logarithmic scaling of the mutual information I_1 for LRHO for a system with periodic boundary condition and configuration $\mathfrak{C}_2$. (Inset) The same quantity for system with boundary and configuration $\mathfrak{C}_4$.

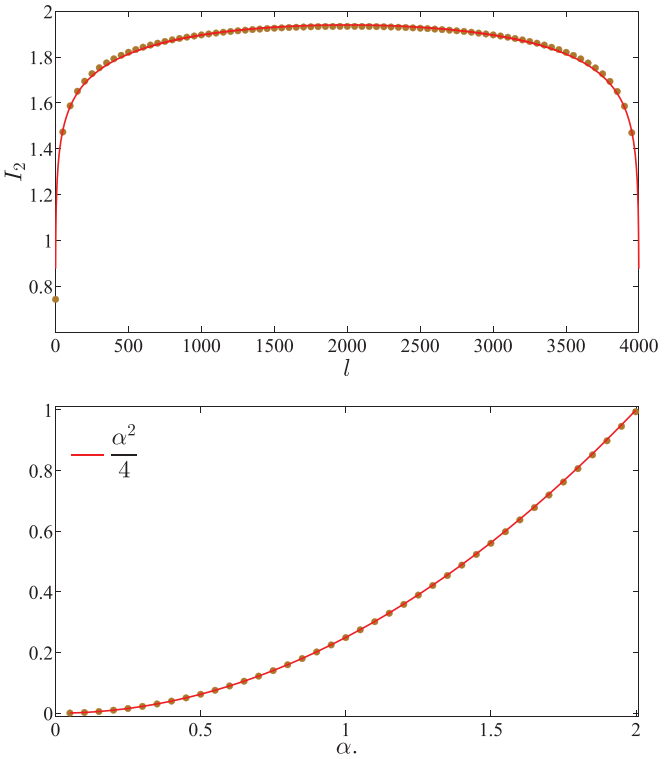

FIG. 23. (Color online) (Top) Mutual information for LRHO ($\alpha = 1.0$) with the configuration $\mathfrak{C}_2$. The solid line represents $I_2 = \frac{1}{8}\ln(l(L-l)) + c_0'$. (Bottom) The prefactor of the logarithmic scaling of the mutual information I_2 for LRHO for a system with periodic boundary condition and configuration $\mathfrak{C}_2$ when $l = L/2$.

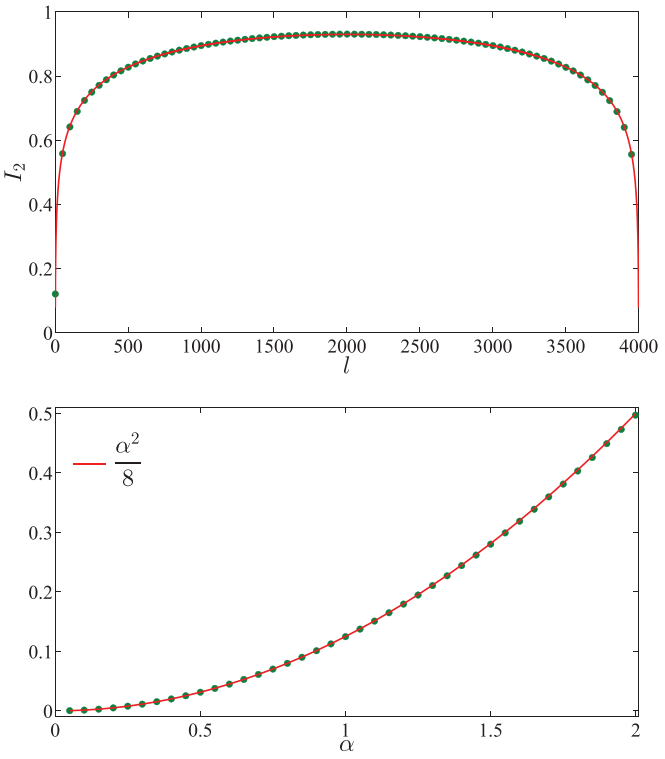

FIG. 24. (Color online) (Top) Mutual information for LRHO ($\alpha = 1.0$) with the configuration $\mathfrak{C}_3$. The solid line represents $I_2 = \frac{1}{8}\ln[l(L-l)] - \frac{1}{8}\ln(L) + c_0'$. (Bottom) The prefactor of the logarithmic scaling of the mutual information I_2 for LRHO with configuration $\mathfrak{C}_4$.

length L with periodic boundary condition. It is then natural to expect that the mutual information I_2 [see Eq. (65)] for systems with finite size, obeys the following formula:

$$I_2 = \frac{\alpha^2}{8}\ln[l(L-l)] + c_0'. \tag{70}$$

We notice that the logarithmic scaling (67) can be recovered from Eq. (70) for $l \ll L$. The numerical computation of the mutual information I_2 in this case can be easily achieved using Eq. (65). The results are shown in Fig. 23 obtaining excellent agreement between the numerical data and Eq. (70).

The mutual information I_2 for a system with periodic boundary condition and subsystem with size $l = L/2$ changes logarithmically as

$$I_2 = \frac{\alpha^2}{4}\ln L + c_0'. \tag{71}$$

The numerical results are shown in Fig. 23. We obtain good agreement with the available theoretical prediction.

We also studied I_2 [see Eq. (65)] for the long-range harmonic oscillator with configuration $\mathfrak{C}_3$. Here, we examine the behavior of the mutual information I_2 for harmonic oscillator with long-range interaction, when the system has boundary. The boundary breaks translational symmetry and it is not therefore possible to use the method followed in Ref. 27. However, it is possible to find the K matrix and then we can use numerical diagonalization of the matrix $K|_A K^{-1}|_A$ to find the eigenvalues and calculate the mutual information I_2. In this case, we observe that

$$I_2 = \frac{\alpha^2}{8}\ln[l(L-l)] - \frac{\alpha^2}{8}\ln(L) + c_0', \tag{72}$$

where in our numerical simulations, we found good agreement with our prediction (see Fig. 24). It is interesting to note that the mutual information I_2 for LRHO with configuration $\mathfrak{C}_4$ grows logarithmically with L:

$$I_2 = \frac{\alpha^2}{8}\ln L + c_0, \tag{73}$$

where this simple behavior is expected from Eq. (72) when $l = L/2$. In Fig. 24, we show our numerical results for the prefactor of the logarithmic term of the mutual information.

B. Massive systems

In this section, we consider massive LRHO with $M > 0$ (configuration $\mathfrak{C}_5$). For the massive case, we study the behavior of the mutual information I_1 and I_2 numerically. It is interesting to note that the mutual information I_1 and I_2 increase logarithmically with the mass and obey the following formula:

$$I_1 = -\frac{\alpha^2}{16}\ln M, \quad I_2 = -\frac{\alpha^2}{4}\ln M. \tag{74}$$

In Fig. 25, we report the results of the simulation of the mutual information I_1 and I_2 for the massive LRHO, where

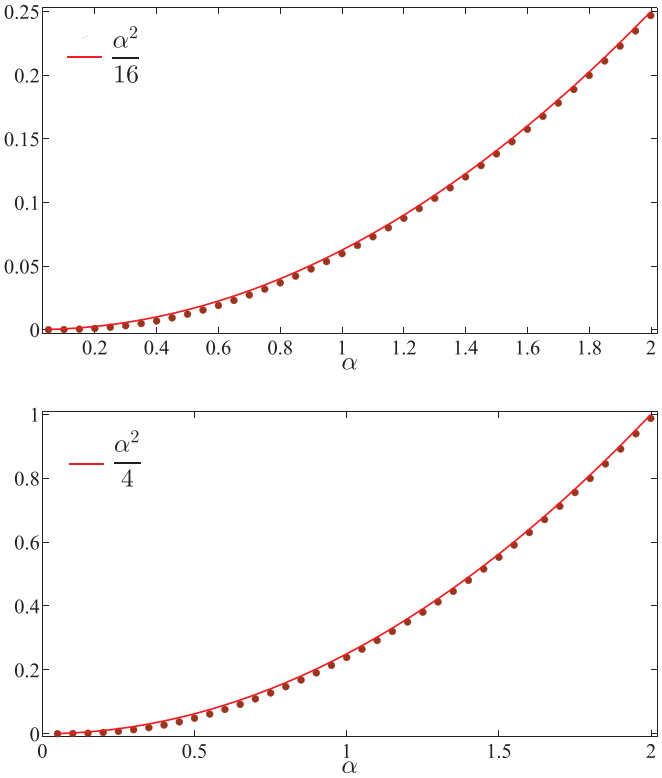

FIG. 25. (Color online) (Top) Prefactor of the logarithmic scaling of the mutual information I_1 for massive LRHO with configuration $\mathfrak{C}_5$. (Bottom) The same quantity for the mutual information I_2.

we calculated the prefactor of the logarithm, which is in good agreement with Eq. (74).

C. Generalized singular Toeplitz matrices

In this section, we generalize our results to the general Toeplitz matrices that we have studied in Sec. III F2. For I_1, the discussion follows the argument given in Ref. 27, which is based on the Fisher-Hartwig theorem. It is very simple to see that since P_A and X_A are Topelitz matrices, for $\alpha_r < 2$, one can simply get the following results for the prefactor of the logarithm of the mutual information $\tilde{c_{I_1}}$ of the subsystem:

$$\begin{aligned}\tilde{c}_{I_1}(\alpha_1,\alpha_1,\alpha_3,\alpha_3,\ldots,\alpha_R) &= \tilde{c}_{I_1}(\alpha_1,\alpha_1,\ldots,0)+\tilde{c}_{I_1}(0,0,\alpha_2,\alpha_2,\ldots,0)\\ &\quad+\cdots+\tilde{c}_{I_1}(0,0,\ldots,\alpha_{R-1},\alpha_{R-1}).\end{aligned} \tag{75}$$

TABLE II. Numerical values of the prefactor $\tilde{c}_{I_1}$ for different values of α_r and q_r.

q_1	q_2	q_3	q_4	q_5	q_6	α_1	α_2	α_3	α_4	α_5	α_6	$\tilde{c}_{I_1}/2$
$\frac{\pi}{3}$	$\frac{-\pi}{3}$	0	0	0	0	1	1	0	0	0	0	0.059(0.001)
$\frac{\pi}{6}$	$\frac{-\pi}{6}$	0	0	0	0	1	1	0	0	0	0	0.059(0.001)
0	0	$\frac{\pi}{3}$	$\frac{-\pi}{3}$	0	0	0	0	1.5	1.5	0	0	0.13(0.01)
0	0	0	0	$\frac{\pi}{3}$	$\frac{-\pi}{3}$	0	0	0	0	2	2	0.24(0.01)
$\frac{\pi}{3}$	$\frac{-\pi}{3}$	$\frac{\pi}{6}$	$\frac{-\pi}{6}$	0	0	1	1	1.5	1.5	0	0	0.19(0.01)
$\frac{\pi}{3}$	$\frac{-\pi}{3}$	$\frac{\pi}{6}$	$\frac{-\pi}{6}$	0	0	1	1	1.5	1.5	2	2	0.44(0.02)
$\frac{\pi}{3}$	$\frac{-\pi}{3}$	$\frac{\pi}{6}$	$\frac{-\pi}{6}$	$\frac{\pi}{4}$	$\frac{-\pi}{4}$	1	1	1.5	1.5	2	2	0.44(0.02)

TABLE III. Numerical values of the prefactor $\tilde{c}_{I_2}$ for different values of α_r and q_r.

q_1	q_2	q_3	q_4	q_5	q_6	α_1	α_2	α_3	α_4	α_5	α_6	$\tilde{c}_{I_2}/2$
$\frac{\pi}{3}$	$\frac{-\pi}{3}$	0	0	0	0	1	1	0	0	0	0	0.125(0.001)
$\frac{\pi}{6}$	$\frac{-\pi}{6}$	0	0	0	0	1	1	0	0	0	0	0.125(0.001)
0	0	$\frac{\pi}{3}$	$\frac{-\pi}{3}$	0	0	0	0	1.5	1.5	0	0	0.27(0.01)
0	0	0	0	$\frac{\pi}{3}$	$\frac{-\pi}{3}$	0	0	0	0	2	2	0.48(0.01)
$\frac{\pi}{3}$	$\frac{-\pi}{3}$	$\frac{\pi}{6}$	$\frac{-\pi}{6}$	0	0	1	1	1.5	1.5	0	0	0.39(0.01)
$\frac{\pi}{3}$	$\frac{-\pi}{3}$	$\frac{\pi}{6}$	$\frac{-\pi}{6}$	0	0	1	1	1.5	1.5	2	2	0.88(0.02)
$\frac{\pi}{3}$	$\frac{-\pi}{3}$	$\frac{\pi}{6}$	$\frac{-\pi}{6}$	$\frac{\pi}{4}$	$\frac{-\pi}{4}$	1	1	1.5	1.5	2	2	0.88(0.02)

A similar result has been already announced in Ref. 27 for the mutual information of a periodic system with half of the system as the subsystem for $\alpha =$ even. We numerically checked the above result in Table II. It is worth mentioning that the prefactors are independent of $b(q)$ and q_r's.

It is not difficult to show that the same formula is also valid for the cases with boundary.

Finally, we should mention that the above argument works perfectly also for I_2. The results of the numerical calculations are shown in Table III for the large system with the small subsystem A.

D. Two dimensions: area law and logarithmic term for polygonal region

In this section, we study the behavior of the Shannon mutual information in two dimensions. Since I_1 is nothing except the $n = 2$ Rényi entanglement entropy, one just expects that Eq. (57) be valid also for this case. In this section, we mostly concentrate on I_2. We first confirmed that the area law is valid also in this case for different values of $\alpha = 2, 1.5$, and 1. Then we checked the effect of sharp corner as we did in the case of entanglement entropy. The best fit for the data is

$$I_2(\theta) = b_0 + b_1 L + b_{-1}L^{-1} + b_{-2}L^{-2} - i(\theta,\alpha)\log L, \tag{76}$$

where θ as before is the vertex angle. The coefficient of the area term is a nonuniversal quantity and increases with α, see Fig. 26. similar to what we had in the case of the entanglement entropy, the coefficient of the logarithm is a universal function and increases with α and decreases with θ, see Fig. 26. It is

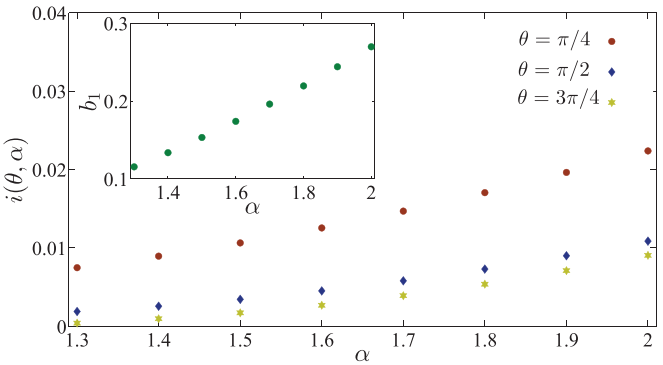

FIG. 26. (Color online) $i(\theta,\alpha)$ as a function of α for subsystems with different vertex angles θ. (Inset) Nonuniversal coefficient of the area term b_1 with respect to different values of α.

worth mentioning that we also calculated the same quantity for I_1 and we found that $i(\theta,\alpha)$ is $\frac{1}{4}$ of the result for I_2.

V. CONCLUSIONS AND DISCUSSIONS

In this paper, we studied the quantum entanglement entropy of coupled long-range harmonic oscillators. We showed that the von Neumann and Rényi entanglement entropy of a subsystem of an infinite system changes logarithmically with the subsystem size, which has a prefactor dependent on the fractional power of the interaction α. We also studied the same quantities in the presence of different kinds of boundary conditions and found that the entanglement entropy changes logarithmically with the subsystem size but with a prefactor that is different from the case without a boundary. The prefactor is interestingly the same as the prefactor coming from the massive case. Having the above results, we concluded that there are just two universal prefactors in our system. Later, we extended our results to the finite temperature case and found a $T^{\frac{2}{\alpha}}$ dependence of the entanglement entropy on the temperature. Our main result was studying the universality of our results by changing the interactions. For example, we considered long-range HO plus short-rang HO and found that the short-range interaction does not have any effect as far as $\alpha < 2$. For $\alpha > 2$, the result is the same as the short-range interaction. We also showed that one can change some other parameters in the interaction and get always the same results. We generalized our findings by studying general singular Toeplitz-like couplings, which in this case we showed that one can calculate the entanglement entropy by just having the results for the simple cases that we have studied. Although in this case we were able to prove the result for the $n = 2$ Rényi case, proving it for the von Neumann entanglement entropy is far from obvious. We also generalized our findings to two-dimensional cases and showed that despite the long-range nature of the couplings, the area law is valid in this case. In addition, we showed that universal logarithmic terms will appear if we consider regions with sharp corner in our system. Finally, we also studied mutual Shannon entropy in our system. We used two definitions; one coming from purely classical considerations and the other comes from using the ground state of the quantum system as the source of probabilities. We showed that the latter case is actually equal to the $n = 2$ Rényi entanglement entropy and one can calculate many things analytically by using the Fisher-Hartwig theorem for Toeplitz matrices. We also provided many simple exact results by using the same method. The generalization to the singular Toeplitz matrices is immediate in these two cases and one can prove that the decomposition mentioned in the case of von Neumann entropy is valid also in this case. There are many other directions that one can extend our work, among the immediate ones, one can mention the study of our system in the presence of the quantum quench, the other direction is studying the entanglement entropy of excited states. Another important study can be investigating the entanglement entropy of long-range Ising model in the mean-field regime where one can relate it to the field theory that we have studied in this paper. We hope to be able to come back to some of these questions in future.

ACKNOWLEDGMENTS

MGN thanks R. Metzler for supports and A. Chechkin for helpful discussions. MGN acknowledges financial support from University of Potsdam. MAR thanks FAPESP for financial support.

APPENDIX: FISHER-HARTWIG THEOREM

The Fisher-Hartwig conjecture, which was proved later by Widom,[43] is about the asymptotic behavior of the determinants of a certain class of Toeplitz matrices. The singular Toeplitz matrices have the following form:

$$K_{l,m} = -\int_0^{2\pi} \frac{dq}{2\pi} e^{iq(l-m)} b(q)\phi(q-q_r), \tag{A1}$$

where $b(q) : S^1 \to \mathcal{C}$ is a smooth nonvanishing function with zero winding number and

$$\phi(q) = \prod_{r=1}^{R} u(\alpha_r,q)t(\beta_r,q), \tag{A2}$$

$$u(\alpha,q) = (2-2\cos q)^{\frac{\alpha}{2}}, \quad \mathrm{Re}\alpha > -1, \tag{A3}$$

$$t(\beta,q) = \exp[-i\beta(\pi-q)], \quad 0 < q < 2\pi. \tag{A4}$$

Fisher and Hartwig conjectured that the determinant of the matrix K follows

$$D_n[K] \sim E G^n(b) n^{\sum_r (\frac{\alpha_r^2}{4}-\beta_r^2)}, \tag{A5}$$

where E is a constant and $G(b) = \exp(\frac{1}{2\pi}\int_0^{2\pi} \log b(q) dq)$. In our study, we took the cases with $\beta_r = 0$, however, we believe that generalizations to $\beta \neq 0$ are straightforward.

*rajabpour@ursa.ifsc.usp.br

[1] L. Amico, R. Fazio, A. Osterloh, and V. Vedral, Rev. Mod. Phys. **80**, 517 (2008).
[2] K. Modi, A. Brodutch, H. Cable, T. Paterek, and V. Vedral, Rev. Mod. Phys. **84**, 1655 (2012).
[3] J. Eisert, M. Cramer, and M. B. Plenio, Rev. Mod. Phys. **82**, 277 (2010).
[4] P. Calabrese and J. Cardy, J. Phys. A **42**, 504005 (2009).
[5] H. Casini and M. Huerta, J. Phys. A **42**, 504007 (2009).
[6] I. Peschel and V. Eisler, J. Phys. A: Math. Theor. **42**, 504003 (2009).
[7] L. Bombelli, R. K. Koul, J. Lee, and R. D. Sorkin, Phys. Rev. D **34**, 373 (1986).
[8] M. Srednicki, Phys. Rev. Lett. **71**, 666 (1993).
[9] C. Callan and F. Wilczek, Phys. Lett. B **333**, 55 (1994).
[10] I. Peschel, J. Phys. A: Math. Gen. **36**, L205 (2003).
[11] O. A. Castro-Alvaredo and B. Doyon, J. Phys. A **42**, 504006 (2009).
[12] J. I. Latorre, R. Orús, E. Rico, and J. Vidal, Phys. Rev. A **71**, 064101 (2005); T. Barthel, S. Dusuel, and J. Vidal, Phys. Rev. Lett. **97**, 220402 (2006); J. Vidal, S. Dusuel, and T. Barthel,

J. Stat. Mech. (2007) P01015; S. Dusuel and J. Vidal, Phys. Rev. B **71**, 224420 (2005).
[13]R. Orus, S. Dusuel, and J. Vidal, Phys. Rev. Lett. **101**, 025701 (2008); M. Filippone, S. Dusuel, and J. Vidal, Phys. Rev. A **83**, 022327 (2011).
[14]W. Dür, L. Hartmann, M. Hein, M. Lewenstein, and H. J. Briegel, Phys. Rev. Lett. **94**, 097203 (2005).
[15]T. Koffel, M. Lewenstein, and L. Tagliacozzo, Phys. Rev. Lett. **109**, 267203 (2012).
[16]J. Eisert and T. J. Osborne, Phys. Rev. Lett. **97**, 150404 (2006); S. Bravyi, M. B. Hastings, and F. Verstraete, *ibid.* **97**, 050401 (2006).
[17]M. B. Plenio, J. Eisert, J. Dreißig, and M. Cramer, Phys. Rev. Lett. **94**, 060503 (2005).
[18]M. Cramer, J. Eisert, M. B. Plenio, and J. Dreißig, Phys. Rev. A **73**, 012309 (2006).
[19]K. Audenaert, J. Eisert, M. B. Plenio, and R. F. Werner, Phys. Rev. A **66**, 042327 (2002); C. H. Bennett, D. P. DiVincenzo, J. A. Smolin, and W. K. Wootters, *ibid.* **54**, 3824 (1996).
[20]A. Botero and B. Reznik, Phys. Rev. A **70**, 052329 (2004).
[21]M. Cramer and J. Eisert, New J. Phys. **8**, 71 (2006).
[22]A. Cadarso, M. Sanz, M. M. Wolf, J. I. Cirac, and D. Perez-Garcia, Phys. Rev. B **87**, 035114 (2013).
[23]O. A. Castro-Alvaredo and B. Doyon, Phys. Rev. Lett. **108**, 120401 (2012); P. Sadhukhan and S. M. Bhattacharjee, J. Phys. A: Math. Theor. **45**, 425302 (2012); H. Katsura and Y. Hatsuda, J. Phys. A **40**, 13931 (2007); D. Giuliano, A. Sindona, G. Falcone, F. Plastina, and L. Amico, New J. Phys. **12**, 025022 (2010); Philippe Corboz and Frederic Mila, arXiv:1212.2983; Shaon Sahoo, V. M. L. Durga, Prasad Goli, S. Ramasesha, and Diptiman Sen, J. Phys.: Condens. Matter **24**, 115601 (2012); Rebecca Ronke, Tim Spiller, and Irene DÁmico, J. Phys.: Conf. Ser. **286**, 012020 (2011).
[24]M. G. Nezhadhaghighi and M. A. Rajabpour, Europhys. Lett. **100**, 60011 (2012).
[25]T. Blanchard, M. Picco, and M. A. Rajabpour, Europhys. Lett. **101**, 56003 (2013).
[26]A. Zoia, A. Rosso, and M. Kardar, Phys. Rev. E **76**, 021116 (2007).
[27]R. G. Unanyan and M. Fleischhauer, Phys. Rev. Lett. **95**, 260604 (2005).
[28]C. Holzhey, F. Larsen, and F. Wilczek, Nucl. Phys. B **424**, 443 (1994).
[29]J. Eisert and M. Cramer, Phys. Rev. A **72**, 042112 (2005); R. Orus, J. I. Latorre, J. Eisert, and M. Cramer, *ibid.* **73**, 060303 (2006).
[30]Ingo Peschel and Jize Zhao, J. Stat. Mech. (2005) P11002.
[31]P. Calabrese and J. Cardy, J. Stat. Mech. (2004) P06002.
[32]P. Calabrese, J. Cardy, and I. Peschel, J. Stat. Mech. (2010) P09003.
[33]J. C. Xavier and F. C. Alcaraz, Phys. Rev. B **85**, 024418 (2012).
[34]S. G. Samko, A. A. Kilbas, and O. I. Marichev, *Fractional Integrals and Derivatives Theory and Applications* (Gordon and Breach, New York, 1993); M. Ilic, F. Liu, I. Turner, and V. Anh, Fract. Calc. Appl. Anal. **8**, 323 (2005).
[35]B. Swingle and T. Senthil, Phys. Rev. B **87**, 045123 (2013).
[36]H. Casini and M. Huerta, Nucl. Phys. B **764**, 183 (2007).
[37]M. M. Wolf, F. Verstraete, M. B. Hastings, and J. I. Cirac, Phys. Rev. Lett. **100**, 070502 (2008).
[38]Jean-Marie Stéphan, Shunsuke Furukawa, Grégoire Misguich, and Vincent Pasquier, Phys. Rev. B **80**, 184421 (2009).
[39]Jean-Marie Stéphan, Grégoire Misguich, and Vincent Pasquier, Phys. Rev. B **82**, 125455 (2010); **84**, 195128 (2011); Michael P. Zaletel, Jens H. Bardarson, and Joel E. Moore, Phys. Rev. Lett. **107**, 020402 (2011).
[40]J. Wilms, M. Troyer, and F. Verstraete, J. Stat. Mech. (2011) P10011; J. Wilms, J. Vidal, F. Verstraete, and S. Dusuel, *ibid.* (2012) P01023.
[41]Jaegon Um, Hyunggyu Park, and Haye Hinrichsen, J. Stat. Mech. (2012) P10026.
[42]F. C. Alcaraz and M. A. Rajabpour, Phys. Rev. Lett. **111**, 017201 (2013).
[43]H. Widom, Am. J. Math. **95**, 333 (1973).
[44]For more subtle finite size effect see Refs. 32 and 33.